

收稿日期：2020-05-06  
改回日期：2020-06-27

基金项目：中国地质调查局地质调查项目“整装勘查区找矿预测与技术应用示范”子项目“吉林省白山市板石沟铁矿区金及铁矿整装勘查区矿产调查与找矿预测”(121201004000172201-06)资助。

doi: 10.12029/gc2020Z203

论文引用格式：吴玉诗, 王海建, 车海龙, 赵虹旭, 马录录, 李爱民, 刘臣臣, 孙冬雪, 马铭, 李东宇. 2020. 吉林省浑江市幅 1:50 000 水系沉积物测量原始数据集 [J]. 中国地质, 47(S2):31-44.

数据集引用格式：吴玉诗; 王海建; 车海龙; 赵虹旭; 马录录. 吉林省浑江市幅 1:50 000 水系沉积物测量原始数据集 (V1). 吉林省第四地质调查所 [ 创建机构 ], 2018. 全国地质资料馆 [ 传播机构 ], 2020-12-30. 10.35080/data.C.2020.P23; <http://dcc.cgs.gov.cn//geologicalData/details/doi/10.35080/data.C.2020.P23>

# 吉林省浑江市幅 1:50 000 水系沉积物 测量原始数据集

吴玉诗 王海建 车海龙 赵虹旭 马录录  
李爱民 刘臣臣 孙冬雪 马铭 李东宇

(吉林省第四地质调查所, 吉林 通化 134001)

**摘要：**吉林省浑江市幅 1:50 000 水系沉积物测量共采集 1961 件水系沉积物样品, 采样粒级为-10 目~+80 目, 平均采样密度为 5.1 个/km<sup>2</sup>。采用发射光谱法 (AES)、泡沫塑料吸附石墨炉原子吸收分光光谱法 (GFAAS)、原子荧光法 (AFS) 及等离子体质谱法 (ICP-MS) 分析了 Au、Ag、Cu、Pb、Zn、As、Sb、Bi、Hg、W、Sn、Mo、Cd、Co、Cr、Ni 等 16 种元素, 形成吉林省 1:50 000 浑江市幅水系沉积物测量原始数据集。数据集包含有 1961 件样品以及其 16 元素的原始数据表 1 个 (Excel), MapGIS 格式图集 1 套 (含有 1 张矿产地质图、1 张采样点位图、16 张单元素地球化学图、16 张单元素异常图)。通过本数据集新发现单元素地球化学异常 403 处, 综合异常 24 处, 结合地质、物探、化探、遥感及已有成矿线索圈定金矿找矿靶区 3 处、铜及多金属找矿靶区 2 处。本文数据集为该区域提供了一套基础性的数据资源, 为地质及其他领域应用提供基础地球化学依据。

**关键词：**地球化学数据；水系沉积物测量；数据集；矿产调查工程；浑江市；吉林省  
**数据服务系统网址：**<http://dcc.cgs.gov.cn>

## 1 引言

吉林省白山市板石沟地区铁及金矿整装勘查区内矿产资源较丰富, 鞍山式铁矿 (洪秀伟等, 2010; 付建飞等, 2014)、热液型金矿 (朱炳玉等, 2011; 王磊等, 2016) 是主要矿产, 另产有铜、铅锌、镁质白云岩、石灰石及煤等。吉林省 90% 以上的贵金属和有色金属矿床都分布在大地构造单元和地质体的边缘部位, 反映“边缘成矿” (孙启祯, 1994) 的特点。近年来图幅北部发现的金英大型金矿, 主要产在金丰度值较高的珍珠门组大理岩中及与底部含砾砂岩类的接触带靠近古陆边缘一侧, 具有明显的层位性。调查区内金英式金矿成矿地质空间广阔, 区域上成矿地质体分布面积大, 地球化学异常与已知控矿构造吻合。

第一作者简介：吴玉诗，男，1977 年生，高级工程师，主要从事地质矿产勘查工作；E-mail: [593483266@qq.com](mailto:593483266@qq.com)。

合程度较好(陈柏林等, 2004), 区内成矿地质条件较好, 找矿潜力较大。但是, 在控矿因素、时空规律、地质历史演化轨迹及区域成矿模式等方面都没有进行过系统有效的研究。涉及本图幅的1:200 000水系沉积物测量工作完成于1983—1986年, 并仅对部分异常进行了查证<sup>①</sup>, 整体工作程度低。通过开展成矿区带1:50 000水系沉积物测量, 查明调查区主要成矿元素地球化学分布和浓集特征, 缩小找矿靶区和查证重要找矿异常, 为资源潜力评价和成矿基础地质研究提供依据(李随民等, 2009)。

吉林省1:50 000浑江市幅图幅区是华北(陆块)成矿省(II-14)、辽东(隆起)铁-铜-铅-锌-金-铀-硼-菱镁矿-滑石-石墨-金刚石成矿带(III-56)(宋相龙等, 2017)的一部分, 横跨铁岭-靖宇(次级隆起)铁-金-铜-铅-锌-石膏成矿亚带(III-56-①)中的四方山-板石铁找矿远景区(V29)和营口-长白(次级隆起、Pt<sub>1</sub>裂谷)铅-锌-铁-金-银-铀-硼-菱镁矿-滑石成矿亚带(III-56-②)中大安金-铁-铜-磷找矿远景区(V31)<sup>②</sup>(图1)。

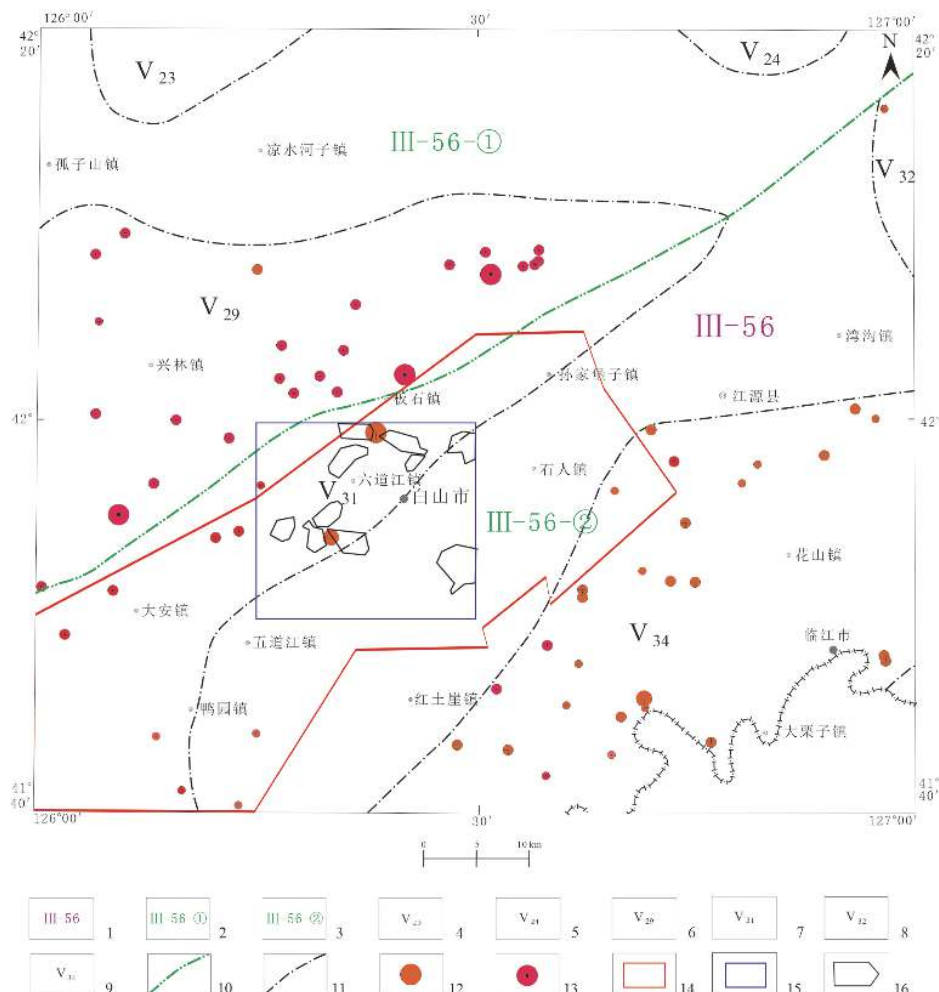


图1 吉林省白山市板石沟地区铁及金矿整装勘查区所属成矿区带位置图

1—III-56 辽东(隆起)铁-铜-铅-锌-金-铀-硼-菱镁矿-滑石-石墨-金刚石成矿带; 2—III-56-① 铁岭-靖宇(次级隆起)铁-金-铜-铅-锌-石膏成矿亚带; 3—III-56-② 营口-长白(次级隆起、Pt<sub>1</sub>裂谷)铅-锌-铁-金-银-铀-硼-菱镁矿-滑石成矿亚带; 4—V23 辉南-抚民金铁找矿远景区; 5—V24 王家店-那尔隆金铜铁镍找矿远景区; 6—V29 四方山-板石铁找矿远景区; 7—V31 大安金铁铜磷找矿远景区; 8—V32 抚松铅锌找矿远景区; 9—V34 南岔-荒沟山金银铁铜铅锌硫找矿远景区; 10—IV級成矿区带界线; 11—V級成矿区带界线; 12—金矿床及矿点; 13—铁矿床及矿点; 14—吉林省白山市板石沟地区铁及金矿整装勘查区范围; 15—浑江市幅工作范围; 16—找矿靶区圈定范围

区域内地质构造错综复杂,经历了古地块形成、盖层发展及大陆边缘活动阶段<sup>③</sup>(潘桂棠等,2009;刘训等,2015)。太古宙至中生界均有不同程度的出露,不同地质单元界面、不同建造单元接触界面往往是构造薄弱地带,为岩浆热液活动提供良好的通道,是成矿的有利部位(图2;王来云等,2010;张万益等,2013)。

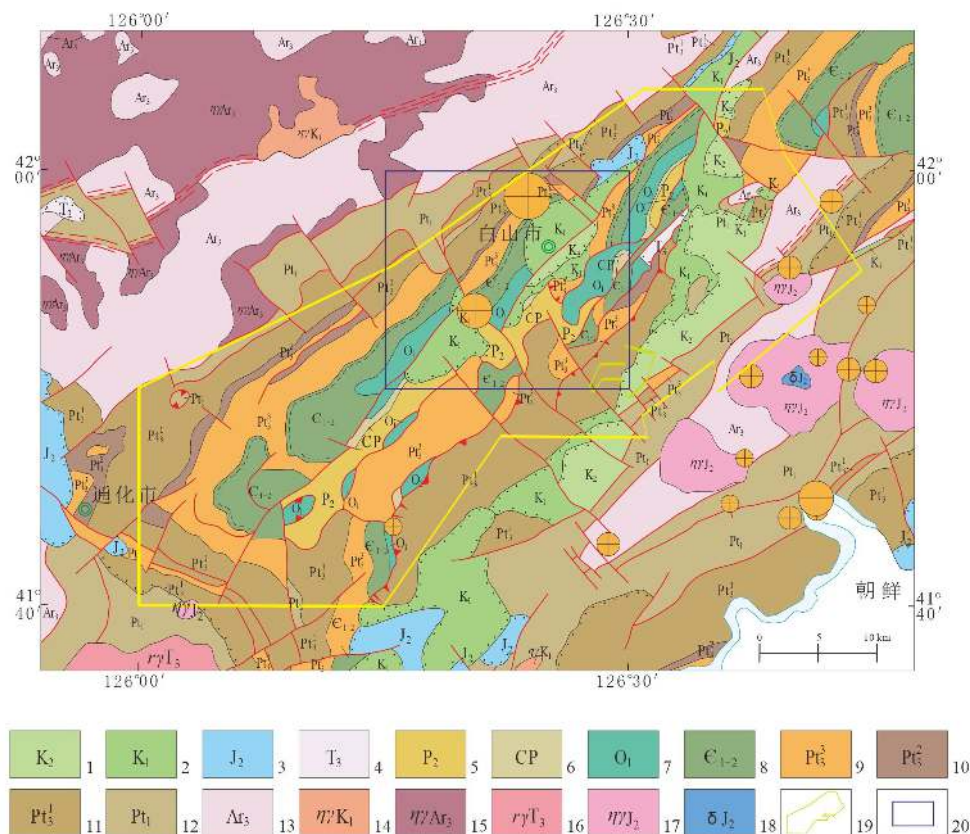


图2 吉林省白山市板石沟地区铁及金矿整装勘查区区域地质简图  
1—白垩系上统;2—白垩系下统;3—侏罗系中统;4—三叠系上统;5—二叠系中统;6—石炭—二叠系;7—奥陶系下统;  
8—寒武系下统—中统;9—震旦系;10—南华系;11—青白口系;12—古元古界;13—新太古界变质表壳岩;14—早白  
垩世二长花岗岩;15—新太古代二长花岗岩;16—晚三叠世二长花岗岩;17—中侏罗世二长花岗岩;18—中侏罗世  
闪长岩;19—吉林省白山市板石沟地区铁及金矿整装勘查区范围;20—浑江市幅工作范围

中国地质调查局整装勘查区找矿预测与技术应用示范“吉林省白山市板石沟地区铁及金矿整装勘查区矿产调查与找矿预测”子项目从2018年5月开始至2018年12月结束,完成了1:50 000浑江市幅水系沉积物测量384 km<sup>2</sup>、1:50 000矿产地质专项填图384 km<sup>2</sup>、1:50 000高精度磁法测量364 km<sup>2</sup>、遥感解译384 km<sup>2</sup>、槽探200 m<sup>3</sup>、综合检查2处、整装勘查区进展跟踪1项等工作量。依托子项目形成吉林省1:50 000浑江市幅水系沉积物测量原始数据集(吴玉诗等,2020;表1)。

## 2 数据采集及处理方法

### 2.1 方法选择

工作区属东北森林沼泽景观区(I)吉林省中部丘陵、低中山森林景观亚区(II)通化市中低山森林景观小区(II<sub>3</sub>),夏、秋季湿润、多雨、剥蚀强、切割深,以物理风化为主,适合开展水系沉积物测量(奚小环等,2012)。根据《地球化学普查规范(1:50 000)》

表1 数据库(集)元数据简表

| 条目       | 描述  |
|----------|---|
| 数据库(集)名称 | 吉林省浑江市幅1:50 000水系沉积物测量原始数据集   |
| 数据库(集)作者 | 吴玉诗,吉林省第四地质调查所<br>王海建,吉林省第四地质调查所<br>车海龙,吉林省第四地质调查所<br>赵虹旭,吉林省第四地质调查所<br>马录录,吉林省第四地质调查所                                    |
| 数据时间范围   | 2018.05—2018.12   |
| 地理区域     | 吉林省1:50 000浑江市幅,位于吉林省东南部,吉林省白山市板石沟地区铁及金矿整装勘查区中部,面积384 km <sup>2</sup> 。地理坐标: E126°15'00"~126°30'00"; N41°50'00"~42°00'00" |
| 数据格式     | *.xlsx, *.wt, *.wl, *.wp  |
| 数据量      | 75.7 MB   |
| 数据服务系统网址 | <a href="http://dcc.cgs.gov.cn">http://dcc.cgs.gov.cn</a>   |
| 基金项目     | 中国地质调查局地质调查项目“整装勘查区找矿预测与技术应用示范(121201004000172201)”子项目“吉林省白山市板石沟地区铁及金矿整装勘查区矿产调查与找矿预测(121201004000172201-06)”              |
| 语种       | 中文  |
| 数据库(集)组成 | 本数据集包括1个Excel数据表,为1961件样品×16种元素的原始分析数据;1个MapGIS图集,内含有1张矿产地质图、1张采样点位图、16张单元素地球化学图、16张单元素异常图                                |

(DZ/T0011-2015),结合调查区地球化学景观特点,确定本次地球化学普查采样介质为水系沉积物,采样密度为4~8点/km<sup>2</sup>,样品粒级选择-10目~+80目。采样点布设在一级水系口、二级水系内,三级水系适当布设控制点。

## 2.2 采样密度

设计采样点密度在一般工作区为4个点/km<sup>2</sup>,重点成矿区带为6~8个点/km<sup>2</sup>,在水系不发育的河谷阶地、山前平原和风积区,按1~2个点/km<sup>2</sup>控制,实际采集水系沉积物样品1961个,平均采样密度5.1个/km<sup>2</sup>。

## 2.3 样品采集

### 2.3.1 野外定点

水系沉积物布点采用1:50 000标准幅地形图为底图,投影类型为“高斯-克吕格(横切椭圆柱等角)投影”,椭球参数为“2000国家大地坐标(CGCS 2000)”。采用安装于UG-9系列掌内的数字填图系统(DGSS),结合地形图进行野外定点(李超龄等,2002;郭福生等,2012)。采样前根据省测绘局基准点,对每个手持掌上机进行定点校验,定点实际距离误差均小于30 m,即在手图上小于0.6 mm,满足《地球化学普查规范(1:50 000)》(DZ/T0011-2015)规定的野外定点误差小于50 m的要求。

### 2.3.2 采样部位

在水系发育区域,采样点选择在水系、沟谷底部,或者是各种粒级冲积物汇集处,譬如水流变缓处、水流停滞处、河道转弯内侧、大石头背后等部位(张永强等,2019)。在羽状水系分布地区,采用一个单元格内多条并列水系采集组合成一个样品;在间隙性流水、干沟或干河道中,选取河床底部采集中细粒物质,排除风成物干扰。

在地表径流不明显或无典型径流的细小水系或者山前水系采集样品时, 样品采集于较大的水系, 沿径流方向有效采集。

水系欠发育区(包括花岗岩风化区、明显的凹型地貌景观区)采样时, 按照凹型地貌中线确定水线, 以此为中心, 向两侧横截宽缓的负地形面等距采集3~5个土壤样品(智云宝等, 2019)。

采样时均按设计位置采集, 局部微调不影响其样品控制范围, 增点、弃点或变更点均进行登记。

### 2.3.3 采样物质

水系发育区域, 采样介质以冲洪积物中粗粒砂、岩屑为主。为提高每个样品的代表性, 在采样点附近30m范围内进行多点(3~5处)采集。

水系欠发育地区, 采用土壤代替水系的方法采集多点组合的样品。采集部位为B层以下、C层以上的残积物质, 采样介质以代表原生地质找矿信息的基岩物质成分为原则。

野外采集原始样品重量>500 g, 最终筛分出的样品重量≥300 g, 满足送检样品和留存副样重量均大于150 g的要求。

## 2.4 样品加工

样品加工基本流程为: 自然干燥→揉匀或敲碎→过筛→拌匀→称重→装袋→装箱→送检。

①样品干燥方式为自然风干。干燥过程中经常揉搓、木棒轻敲, 以免结块, 雨季特别注意防止雨淋、风沙或人为因素等造成样品的散失或玷污。

②采用-10目、+80目不锈钢套筛, 对充分干燥后的样品过筛, 弃除筛上及筛下物, 截取样品重量大于300 g。

③按四分法缩分配置分析样品, 分析样品重量150 g, 用牛皮纸袋封装, 剩余150 g样品作为副样封箱留存。

## 2.5 样品分析及测试方法

样品测试分析工作由具备岩矿测试甲级资质的中国建筑材料工业地质勘查中心辽宁测试研究所承担, 严格执行《地球化学普查(比例尺1:50 000)规范样品分析技术的补充规定》(中地调发〔2007〕220号)。

根据项目合同书及年度设计要求, 1:50 000水系沉积物测量分析项目为Au、Ag、Cu、Pb、Zn、As、Sb、Bi、Hg、W、Sn、Mo、Cd、Co、Cr、Ni等16种元素(张江华等, 2013; 赵武强等, 2014)。

实验室通过优化、筛选和研究, 制定了以等离子体质谱法(ICP-MS)为主体, 辅以其他分析方法组成的多种测试手段的分析配套方案(表2), 分析要求检出限与方法检出限满足水系沉积物元素分析测试质量的需要(表3)。

## 2.6 数据处理

本次数据处理软件采用中国地质科学院地球物理地球化学勘查研究所自主研发的地球化学勘查一体化系统(Geochem Studio 3.5.3), 离散数据网格化(300 m×300 m)后, 采用逐步剔除3倍标准离差(3S)的正态分布异常下限后进行数据处理(王新春等, 2016)。

表2 分析方法及配套方案

| 分析方法               | 检验元素                               | 测试精度         |
|--------------------|------------------------------------|--------------|
| 发射光谱法(AES)         | Ag                                 | ≥0.01 nm     |
| 石墨炉原子吸收分光光度法(GFAA) | Au                                 | ≥0.002 nm    |
| 原子荧光法(afs)         | As、Hg                              | ≥0.3 nm      |
| 等离子质谱法(ICP-MS)     | Cr、Co、Ni、Cu、Zn、Mo、Cd、Sn、Sb、W、Pb、Bi | 0.01~10 μg/L |

表3 分析要求检出限与方法检出限对比表

| 序号 | 元素   | 方法检出限  | 要求检出限  | 单位   | 分析方法   |
|----|------|--------|--------|------|--------|
| 1  | Cr 铬 | 10     | 15     | μg/g | ICP-MS |
| 2  | Co 钴 | 0.5    | 1      | μg/g | ICP-MS |
| 3  | Ni 镍 | 2      | 3      | μg/g | ICP-MS |
| 4  | Cu 铜 | 1      | 1.5    | μg/g | ICP-MS |
| 5  | Zn 锌 | 5      | 15     | μg/g | ICP-MS |
| 6  | Mo 钼 | 0.2    | 0.5    | μg/g | ICP-MS |
| 7  | Cd 镉 | 0.1    | 0.1    | μg/g | ICP-MS |
| 8  | Sn 锡 | 0.5    | 1      | μg/g | ICP-MS |
| 9  | Sb 锑 | 0.03   | 0.2    | μg/g | ICP-MS |
| 10 | W 钨  | 0.2    | 0.5    | μg/g | ICP-MS |
| 11 | Pb 铅 | 2      | 5      | μg/g | ICP-MS |
| 12 | Bi 铋 | 0.1    | 0.1    | μg/g | ICP-MS |
| 13 | As 砷 | 0.5    | 1      | μg/g | AFS    |
| 14 | Hg 汞 | 0.005  | 0.0005 | μg/g | AFS    |
| 15 | Ag 银 | 0.02   | 0.03   | μg/g | AES    |
| 16 | Au 金 | 0.0003 | 0.0003 | μg/g | GFAAS  |

### 2.6.1 数据处理

#### (1) 数据分布型式检验

根据数据统计大数定律, 样品数量较多时元素的分布形式趋于正态分布。用剔除大于平均值加3倍标准离差后的数据, 进行了偏度、峰度值检验, 全区16种元素均趋向算术正态分布, 因此, 采用算术平均方法作为确定平均值与离差的依据。

#### (2) 地球化学参数统计计算

对图幅内16种元素的原始数据集, 离散数据网格化( $300\text{ m} \times 300\text{ m}$ )后, 选择剔除异点的正态分布异常下限, 采用逐步剔除3倍标准离差( $3S$ )后数据进行, 直到无离群数值可剔除为止, 形成背景数据集(刘洪等, 2015)。以剔除离群全域均值( $\bar{X}$ )和标准离差( $S$ )为依据计算异常下限( $T$ ), 计算方法为 $T=\bar{X}+1.65S$ , 最终确定异常下限值。

#### (3) 成图数据参数设置

对采样点数据采用距离反比加权插值法处理, 转换适用于制作地球化学图的规则矩形网格数据。距离幂指数2, 采用四方向搜索, 每搜索方向点数6个点, 有效最少数据点数5个点, 最大空方向允许数4个点, 网格间距 $300\text{ m} \times 300\text{ m}$ , 搜索半径2000 m。

本次工作共采集样品1961件, 其中土壤样品101件, 呈零星点分布于采样单元格内, 样品粒级与水系沉积物测量采样粒级保持一致, 数据处理时土壤代替样对结果不造成影响。

### 2.6.2 图件编制

#### (1) 实际材料图

主要内容包括水系、主要居民点、主要地物标志、交通道路、高斯方里网、经纬度坐标、采样点位置及采样信息等属性。重复样点、质量检查点以不同的颜色或符号标注。

#### (2) 元素地球化学图

等值线色区采用《地球化学普查规范(1:50 000)》(DZ/T0011—2015)规定的15级色阶法,用其对应的含量间隔勾绘等量线成图,各色级色阶内不同等量线间隔采用过渡色阶表示,使用同一色阶内相关区带达到渐变效果。

#### (3) 地球化学异常图

根据地球化学图背景分布特征、地质体、构造等特征,将本区分为2个分区,地球化学分区是根据地球化学图和地质图中地质体背景的相互关系而确定,利用分区异常下限求取衬值后,直接圈定异常。

#### (4) 组合异常图

在单元素异常图的基础上,利用Geochem Studio 3.5.3软件,对工作区原始数据进行R型聚类分析和因子分析,根据软件分析结果确定研究对象的元素组合特征,选择3~5个元素编绘等值线(异常线)。同时确定一个主要元素,勾绘异常浓度分级等值线和等值区,等值线分别用规范要求的不同的颜色线条,等值区用面色表示内、中、外带。

#### (5) 成矿预测图

在分析各类地球化学图的基础上,按地质意义、地球化学异常分类评价结果、地球化学异常组合与空间分布规律,结合地质条件等综合因素划定找矿远景区和靶区。

### 3 数据样本描述

吉林省1:50 000浑江市幅水系沉积物测量原始数据集由元素地球化学分析数据表及MapGIS格式图件组成。元素地球化学分析数据类型为字符型与浮点型([向运川等,2018;表4](#))。图件包含实际材料图、元素地球化学图、地球化学异常图、组合异常图及成矿预测图,为MapGIS格式的点、线、面文件组成。MapGIS格式数据类型分为长整型、双精度型、字符型、浮点型([表5、表6、表7](#))。样品中各分析元素属性结构及图件中点、线、面等文件的属性结构均参照中国地质调查局固体矿产勘查数据库内容与结

表4 浑江市幅元素地球化学分析数据表

| 序号 | 字符名称 | 数据类型 | 实例       | 序号 | 字符名称 | 数据类型 | 实例    |
|----|------|------|----------|----|------|------|-------|
| 1  | 分析批号 | 字符型  | 2018化302 | 11 | Bi   | 浮点型  | 0.25  |
| 3  | 矿样号  | 字符型  | HJS001C1 | 12 | Hg   | 浮点型  | 0.034 |
| 4  | Au   | 浮点型  | 1.00     | 13 | W    | 浮点型  | 1.41  |
| 5  | Ag   | 浮点型  | 70.80    | 14 | Sn   | 浮点型  | 2.30  |
| 6  | Cu   | 浮点型  | 16.40    | 15 | Mo   | 浮点型  | 0.84  |
| 7  | Pb   | 浮点型  | 19.40    | 16 | Cd   | 浮点型  | 0.09  |
| 8  | Zn   | 浮点型  | 88.10    | 17 | Co   | 浮点型  | 14.60 |
| 9  | As   | 浮点型  | 6.44     | 18 | Cr   | 浮点型  | 71.20 |
| 10 | Sb   | 浮点型  | 0.57     | 19 | Ni   | 浮点型  | 27.00 |

注:元素含量单位: Au、Hg为ng/g,其他元素为μg/g。

构(李超龄等, 2013; 左群超等, 2018)填写, 数据结构(王杨刚等, 2015; 袁慧香等, 2015)内容完整齐全。

表5 浑江市幅元素地球化学图点元数据特征与类型

| 序号 | 字符名称   | 数据类型 | 实例                        |
|----|--------|------|---------------------------|
| 1  | ID     | 长整型  | 1                         |
| 2  | 异常编号   | 字符串  | Ag-1                      |
| 3  | 位置     | 字符串  | (292 208.88, 4653 922.84) |
| 4  | 异常点数   | 长整型  | 3                         |
| 5  | 异常下限   | 双精度型 | 1                         |
| 6  | 异常面积   | 双精度型 | 0.558 407                 |
| 7  | 异常面积序数 | 长整型  | 7                         |
| 8  | 平均值    | 双精度型 | 1.143 667                 |
| 9  | 平均值序数  | 长整型  | 12                        |
| 10 | 极大值    | 双精度型 | 1.231                     |
| 11 | 极大值序数  | 长整型  | 12                        |
| 12 | 衬度     | 双精度型 | 1.143 667                 |
| 13 | 衬度序数   | 长整型  | 12                        |
| 14 | AD     | 双精度型 | 0.638 632                 |
| 15 | AD序数   | 长整型  | 8                         |
| 16 | AP     | 双精度型 | 0.080 224                 |
| 17 | AP序数   | 长整型  | 11                        |
| 18 | NAD    | 双精度型 | 0.638 632                 |
| 19 | NAD序数  | 长整型  | 8                         |
| 20 | NAP    | 双精度型 | 0.080 224                 |
| 21 | NAP序数  | 长整型  | 8                         |
| 22 | 分带数    | 长整型  | 1                         |

表6 浑江市幅元素地球化学图线元数据特征与类型

| 序号 | 字符名称    | 数据类型 | 实例         |
|----|---------|------|------------|
| 1  | ID      | 长整型  | 1          |
| 2  | 长度      | 双精度型 | 80.556 64  |
| 3  | 高度      | 双精度型 | 1          |
| 4  | 元素编号    | 字符串  | Ag-1       |
| 5  | bh      | 字符串  | Ag-1       |
| 6  | UserID  | 长整型  | -1         |
| 7  | MAPCODE | 字符串  | K52E013002 |
| 8  | CHFCAC  | 字符串  | 1          |
| 9  | YSYCLZ  | 浮点型  | 0.12       |
| 10 | YSYCLX  | 字符串  | 0          |
| 11 | YCTZ    | 字符串  | 0          |
| 12 | YCDZ    | 浮点型  | 0.15       |
| 13 | HLZ     | 浮点型  | 0.08       |

表7 浑江市幅元素地球化学图面元数据特征与类型

| 序号 | 字符名称        | 数据类型 | 实例         |
|----|-------------|------|------------|
| 1  | ID          | 长整型  | 16         |
| 2  | 面积          | 双精度型 | 433.29     |
| 3  | 周长          | 双精度型 | 271.77     |
| 4  | MAPCODE     | 字符串  | K52E013002 |
| 5  | Start_value | 双精度型 | 1          |
| 6  | end_value   | 双精度型 | 2          |

#### 4 数据质量控制和评估

中国建筑材料工业地质勘查中心辽宁测试研究所根据所选用分析元素的配套方法及检出限, 分析方法的准确度和精密度均可以满足《地球化学普查规范 1:50 000》(DZ/T0011-2015) 要求。各元素检出限、报出率等见表8。

表8 分析方法的检出限及分析元素报出率

| 序号 | 被检测元素 | 分析方法的检出限 | 规范要求的检出限 | 报出率/% | 分析方法   |
|----|-------|----------|----------|-------|--------|
| 1  | Au    | 0.0003   | 0.0003   | 100   | GFAAS  |
| 2  | Ag    | 0.02     | 0.03     | 100   | AES    |
| 3  | Cu    | 1.0      | 1.5      | 100   | ICP-MS |
| 4  | Pb    | 2        | 5        | 100   | ICP-MS |
| 5  | Zn    | 5        | 15       | 100   | ICP-MS |
| 6  | As    | 0.5      | 1        | 100   | AFS    |
| 7  | Sb    | 0.03     | 0.2      | 100   | ICP-MS |
| 8  | Bi    | 0.1      | 0.1      | 100   | ICP-MS |
| 9  | Hg    | 0.005    | 0.0005   | 100   | AFS    |
| 10 | W     | 0.2      | 0.5      | 100   | ICP-MS |
| 11 | Sn    | 0.5      | 1        | 100   | ICP-MS |
| 12 | Mo    | 0.2      | 0.5      | 100   | ICP-MS |
| 13 | Cd    | 0.1      | 0.1      | 100   | ICP-MS |
| 14 | Co    | 0.5      | 1        | 100   | ICP-MS |
| 15 | Cr    | 10       | 15       | 100   | ICP-MS |
| 16 | Ni    | 2        | 3        | 100   | ICP-MS |

注:等离子体质谱法(ICP-MS)、原子荧光法AFS、泡沫塑料吸附石墨炉原子吸收法(GFAAS)

质量管理采用外部质量监控和内部质量监控相结合, 以外部质量监控为主的原则, 样品外部监控样按照中国地质调查局要求购买自中国地质科学院地球物理地球化学勘查研究所。外部质量监控样按照样品总数 5% 的比例共插入 100 件; 内部质量监控以每 50 件分样品为 1 个分析组, 插入 4 个监控样; 每 500 件样品中再插入 12 个土壤一级标准物质。对分析方法准确度、精密度、系统误差、偶然误差进行监控, 元素准确度 100%, 精密度可以满足规范要求。

内检样品及异常点质量监控: 内检样品按照样品总数的 8% 进行检查分析。对部分元素含量较高或较低的样品进行异常抽查。各元素的内检分析和异常值抽查的质量控制

均按相对偏差  $RD \leq 25\%$  统计合格率, 一次原始合格率  $\geq 90\%$ 。

为了避免由于分析偶然误差而造成的地球化学假象, 实验室在每批样品分析完毕后, 都对部分分析结果的突变高值点和低值点进行重复性检验。水系异常点抽查的总项数为 1824 项, 总合格项数为 1799 项, 总合格率为 98.63%, 检查比例 6.13%。

水系沉积物内检和异常点抽查总项数为 3008 项, 总合格数为 2962 项, 总合格率为 98.47%, 检查比例为 10.09%。

各类样品分析资料, 由分析单位提供分析报告和资料盘, 经资料处理员核对确认无误后进行资料入库, 入库资料经过多次核对, 确认无误后使用。各类计算均采用相应的计算程序, 以一组标准资料验算后由计算机完成。有关图件、表格的编制、各种资料的引用都做了 100% 的核查, 保证了资料整理工作的正确性、准确性。

## 5 异常圈定及特征

### (1) 异常圈定

单元素异常以地球化学分区所确定的异常下限在微机上直接圈定, 综合异常圈定是在所圈定的各单元素异常的基础上, 结合地质背景、异常元素组合特征、地形地貌因素进行人工干预, 对异常进行分解或适当调整, 部分规模较小的单点异常予以删除(李随民等, 2014)。

根据 16 个主要成矿元素综合异常中各元素异常的规模(NAP)确定图幅内主成矿元素及伴生矿元素(师淑娟等, 2011), 主要以在其全区单元素异常规模排序中靠前的元素且在综合异常中单元素异常规模最大确定。

本次工作共圈定单元素异常 403 个, 综合异常 24 个, 编号为浑浑 18HS-1—浑浑 18HS-24, 分别进行了登记、解释和评序, 共划分出甲<sub>1</sub>类异常 3 个, 乙<sub>2</sub>类异常 7 个, 乙<sub>3</sub>类异常 14 个(表 9)。

其中浑浑 18HS-2 综合异常区中分布有板庙子金矿床(金英金矿), 该矿床是吉林省白山地区一重要的大型岩金隐伏矿床, 在区域上具有代表性, 未来资源潜力较大(王登红, 2016)。因该矿床 1:200 000 化探异常不明显, 通过本次工作确定该矿床的化探主要指示元素(王磊等, 2020)有 Au、Cu、As、Hg、Cd 等, 其中 As 基本上位于内带, Hg、Cu 基本上位于中外带, Au、Cd 位于中外带。其中 As、Sb、Hg、V 为矿体的前缘晕(牛树银等, 2012), 可作为隐伏金矿的找矿标志。图幅北西部分布有类似于板庙子金矿的成矿地质体 60 余平方千米, 且异常套合好, 为寻找该类型金矿的找矿突破提供了充足的地质空间。浑浑 18HS-16 综合异常范围内分布刘家堡子-狼洞沟金银矿床, 该矿床的化探主要指示元素有 Au、Ag、Cu、Pb、Cd、As、Sb、Hg、W、Mo、Bi 等, Sn、W、As、Sb 元素基本位于内带, Cd、Bi 位于中带, Cu、Mo、Au、(Ag) 位于外带。在异常检查工作中新发现含铜花岗闪长斑岩, 具有寻找斑岩型铜金矿的潜力(韦少港等, 2016), 对下一步找矿工作具有重要意义。区内分布有多个与浑浑 18HS-2、浑浑 18HS-16 异常相类似的综合异常, 且成矿地质条件优越(张运强等, 2015; 杨剑等, 2015), 为整装勘查区内低温热液型金及多金属矿(张璟等, 2010; 王成辉等, 2012)、斑岩型铜(金)矿(汪东波等, 2016)的找矿突破提供了有利条件。

通过异常检查, 甲<sub>1</sub>类异常和乙<sub>2</sub>类异常均发现了矿化蚀变体或异常地质体, 且甲<sub>1</sub>类异常中已查明有吉林省白山市金英金矿床、吉林省白山市刘家堡子-狼洞沟金银矿床, 证明了异常评序与评价分类的准确性。

表9 主要成矿元素综合异常特征一览表<sup>①</sup>

| 异常<br>编号  | 元素组合<br>(按规模降序)                          | 规模<br>(NAP) | 成矿主元素及伴生元素<br>(规模)   | 异常<br>类别       |
|-----------|--|-------------|--|----------------|
| 浑浑18HS-1  | Cd–As–Hg–Au–Bi                           | 7.28        | Cd(3.67)   | 乙 <sub>3</sub> |
| 浑浑18HS-2  | Au–Cr–Hg–As–Cd–Cu–Ni                     | 34.20       | Au(22.81) Cr(4.12)   | 甲 <sub>1</sub> |
| 浑浑18HS-3  | Au–Cr–Hg                                 | 13.1        | Au(7.85) Cr(4.77)  | 乙 <sub>3</sub> |
| 浑浑18HS-4  | As–Hg–Sb–Cr–Mo–W–Ni–Ag–Co–Sn–Cu          | 47.76       | Sb(10.69) Cr(5.35) Mo(3.52)<br>W(1.48) Ni(1.41) Ag(1.12) Co(1.03)  | 乙 <sub>2</sub> |
| 浑浑18HS-5  | Cr–Au–Cu–Ni–Sb–Mo–W                      | 33.32       | Cr(13.69) Au(6.75) Cu(4.41)<br>Ni(3.55) Sb(2.57) Mo(1.64)  | 乙 <sub>2</sub> |
| 浑浑18HS-6  | Hg–Sb–Au–W–Mo–Cd–As–Pb                   | 36.77       | Sb(9.45) Au(5.38) W(2.24)<br>Mo(1.96) Cd(1.50)   | 乙 <sub>2</sub> |
| 浑浑18HS-7  | Cr–Mo–Cu–Ni–As–Sb                        | 8.04        | Cr(2.65) Mo(2.23) Cu(2.13) Ni(1.49)  | 乙 <sub>3</sub> |
| 浑浑18HS-8  | Au–Sb–Cr–Hg–W–Cu–As–Mo                   | 48.54       | Au(19.96) Sb(11.73) Cr(7.34)<br>W(2.38)  | 乙 <sub>2</sub> |
| 浑浑18HS-9  | W–Cr–Au–Sb                               | 7.68        | W(2.69) Cr(2.60) Au(1.75)  | 乙 <sub>3</sub> |
| 浑浑18HS-10 | Cr–As–Sb–Bi–Cu–Zn–Pb–Co–Mo–Au–Ni–Sn–Cd   | 41.59       | Cr(12.4) Sb(4.11) Bi(3.24) Cu(2.33)<br>Zn(2.23) Pb(1.75) Co(1.63)<br>Mo(1.43) Au(1.36)                   | 乙 <sub>3</sub> |
| 浑浑18HS-11 | Sb–Mo–W–As–Hg–Cu–Ni                      | 6.49        | Sb(1.38) Mo(1.05) W(1.03)  | 乙 <sub>3</sub> |
| 浑浑18HS-12 | Co–Cr–Mo–Cu–Pb–Sn–Au–Ni–Bi               | 22.74       | Co(10.21) Cr(3.37) Mo(3.30)<br>Cu(2.32) Pb(1.37)   | 乙 <sub>3</sub> |
| 浑浑18HS-13 | Mo–Au–Cu–W–Cd–Sb–Cr–Hg                   | 44.54       | Mo(12.72) Au(7.39) Cu(6.98)<br>W(5.75) Cd(3.92) Sb(3.42) Cr(3.21)  | 乙 <sub>2</sub> |
| 浑浑18HS-14 | Cr–Sb–Mo–Ni–As–Cu–Co–Ag–Cd               | 23.19       | Cr(8.35) Sb(5.19) Mo(2.70) Ni(2.26)  | 乙 <sub>3</sub> |
| 浑浑18HS-15 | Au–Cr–Ag–Cu–Cd–Pb–Bi–Sb–Zn–As–W–Co       | 26.89       | Au(7.23) Cr(4.17) Ag(3.57)<br>Cu(2.80) Cd(2.60) Pb(2.01) Bi(1.21)<br>Sb(1.10)                            | 乙 <sub>2</sub> |
| 浑浑18HS-16 | Au–Ag–Cu–Cr–Cd–Bi–Zn–Pb–Mo–As–Sb–W       | 90.87       | Au(41.68) Ag(9.37) Cu(6.68)<br>Cr(6.20) Cd(6.05) Bi(4.54) Zn(4.53)<br>Pb(4.46) Mo(3.03) Sb(1.17) W(1.00) | 甲 <sub>1</sub> |
| 浑浑18HS-17 | Au–Ag–Cu–Mo–Sb–Hg–As–Cr–Pb–W–Cd–Ni–Sn    | 80.04       | Au(41.68) Ag(6.87) Cu(5.57)<br>Mo(5.40) Sb(5.30) Cr(3.41) Pb(2.01)<br>W(1.42)                            | 甲 <sub>1</sub> |
| 浑浑18HS-18 | Sb–As–Au–Cd–W–Co–Cu                      | 12.04       | Sb(3.37) Au(2.20) Cd(1.61) W(1.14)   | 乙 <sub>3</sub> |
| 浑浑18HS-19 | Cr–Au–Cu–Sn–Hg–Bi                        | 13.59       | Cr(5.70) Au(2.99) Cu(2.88) Sn(1.08)  | 乙 <sub>3</sub> |
| 浑浑18HS-20 | As–Sb–Co–Cr–Au–Ag–Cu–Pb–Cd–Ni–Zn–Hg–Sn–W | 55.60       | Sb(7.41) Co(6.81) Cr(5.79) Au(5.60)<br>Ag(4.32) Cu(3.76) Pb(3.41)<br>Cd(2.84) Ni(2.59) Zn(2.20)          | 乙 <sub>2</sub> |
| 浑浑18HS-21 | Cr–Cu–Ag–Co–Ni–Hg–Pb–Sn–Bi               | 24.87       | Cr(6.95) Cu(4.66) Ag(3.47) Co(3.41)<br>Ni(2.66)  | 乙 <sub>3</sub> |
| 浑浑18HS-22 | W–Hg–Cr–Mo–Au–Bi–As–Sn–Zn–Cu–Pb          | 13.71       | W(3.28) Cr(2.13) Mo(1.27)  | 乙 <sub>3</sub> |
| 浑浑18HS-23 | Pb–As–Cd–Hg–Mo–Cu–Ni                     | 8.75        | Pb(2.18) Cd(1.90)  | 乙 <sub>3</sub> |
| 浑浑18HS-24 | Hg–Sb–Cr–Cd–Cu–Pb–Bi–W–Ni–Co             | 25.83       | Sb(5.32) Cr(4.05) Cd(3.77) Cu(1.75)<br>Pb(1.20)  | 乙 <sub>3</sub> |

## (2) 异常总体特征

地球化学异常分布在空间上具有一定的规律性, 总体展布(轴部)多呈北东向, 受浑江向斜北西翼地层走向控制明显, 局部呈北西向或近东西向。此外, 异常展布方向往往与断裂构造存在一定内在联系, 尤其在北东向断裂、北东向与北西向断裂交汇部位, 多形成分布有规模和强度可观的地球化学异常。

## 6 结论

1:50 000 浑江市幅水系沉积物测量原始数据集客观反映了调查区内各元素的分布规律及地质矿产信息资料, 对区内16种单元素异常和综合异常均进行了评序。共圈定主成矿(指示)元素单元素异常403个, 综合异常24处, 其中甲类3个, 乙类21个。在对全区资源潜力定性评价的基础上, 圈定I级成矿远景区1个, II级成矿远景区1个; A级找矿靶区3个, B级找矿靶区7个。本区成矿类型主要为中(低)温热液型, 主要矿种为金、银、锑、钼、铜、铅、锌等多金属矿床。通过重点异常检查发现铜铅锌银矿化线索两处。结合区域矿产特征, 初步建立了整装勘查区内典型金、金银矿床的地球化学模式对本图幅内后续的找矿工作具有重要的指导意义。

吉林省1:50 000 浑江市幅水系沉积物测量原始数据集的建立为该区域提供了一套基础性的数据资源, 可最大限度地满足科研人员对图幅内水系沉积物测量信息的查询需求, 为实现信息资源共享创造了条件, 为基础地质及其他领域应用提供基础地球化学依据。

致谢: 感谢中国地质调查局发展研究中心对项目的大力支持。

注释:

- ① 王绪忠, 刘景霞, 秦洪莲, 刘玉兰. 1988. 浑江幅(11-52-[19])地球化学图说明书[R]. 九台: 吉林省地质矿产局第五地质调查所. 1-44.
- ② 李任时, 徐曼, 李楠, 马晶, 崔丹, 宋小磊. 2013. 吉林省矿产资源潜力评价化探资料应用成果报告[R]. 长春: 吉林省地质调查院. 285-326.
- ③ 周晓东, 彭玉鲸, 路孝平, 李东津, 王光奇, 潘建, 王彦生, 卢兴波, 邸新, 李福文, 苑凤华, 聂立军, 张艳玲, 曹立敏, 王信. 2019. 中国区域地质志·吉林志[R]. 长春: 吉林省区域地质矿产调查所. 1861-1882.
- ④ 吴玉诗, 王海建, 刘正宏, 车海龙, 马录录, 李爱民, 赵虹旭, 王慧明. 2019. 吉林省白山市板石沟铁矿地区金及铁矿整装勘查区矿产调查与找矿预测子项目成果总报告[R]. 通化: 吉林省第四地质调查所. 1-328.

## 参考文献

- 陈柏林, 李中坚, 董诚, 丁式江, 舒斌, 廖香俊, 董法先, 傅杨荣. 2004. 海南抱伦金矿床控矿构造特征及其对金矿化的控制作用[J]. 中国地质, 31(2): 139-146.
- 付建飞, 王恩德, 夏建明, 门业凯, 陈慧钧, 尤欣慰, 成林. 2014. 辽宁眼前山铁矿元素地球化学特征与沉积古环境研究[J]. 中国地质, 41(6): 1929-1943.
- 郭福生, 吴志春, 谢财富, 刘林清, 姜勇彪, 时国, 周万鹏. 2012. 数字地质填图系统的几点改进意见及实用技巧[J]. 中国地质, 39(1): 252-259.
- 洪秀伟, 庞宏伟, 刘学文, 李尔峰, 王文清, 王长峰, 刘铁. 2010. 辽宁本溪大台沟铁矿地质特征[J]. 中国地质, 37(5): 1426-1433.

- 李超岭, 黄与能, 张克信, 叶天竺, 李丰丹, 刘畅, 龙宝林, 于庆文, 张生辉, 陶继雄, 刘修国, 葛梦春, 吕志成, 朱学立, 徐开锋, 杨东来, 李景朝, 陈春香. 2013. 固体矿产勘查数据库内容与结构 [S]. 北京: 中国地质调查局. 1–319.
- 李超岭, 杨东来, 于庆文. 2002. 数字地质调查与填图技术方法研究 [J]. 中国地质, 2(2): 213–217.
- 李随民, 吴景霞, 栾文楼, 魏明辉, 陈树清. 2009. 地球化学块体方法在冀北金矿资源潜力估算中的应用 [J]. 中国地质, 36(2): 444–449.
- 李随民, 魏明辉, 郝华金. 2014. 消除背景影响的化探异常圈定方法——以张家口地区为例 [J]. 中国地质, 41(6): 2083–2090.
- 刘洪, 黄瀚霄, 李光明, 肖万峰, 张智林, 刘波, 马东方, 董磊, 马东. 2015. 因子分析在藏北商旭金矿床地球化学勘查中的应用 [J]. 中国地质, 42(4): 1126–1136.
- 刘训, 游国庆. 2015. 中国的板块构造区划 [J]. 中国地质, 42(1): 1–17.
- 牛树银, 李凤友, 陈华山, 孙爱群, 王宝德, 王金忠, 马宝军. 2012. 冀东金厂峪金矿深部和外围找矿预测 [J]. 中国地质, 39(4): 999–1006.
- 潘桂棠, 肖庆辉, 陆松年, 邓晋福, 冯益民, 张克信, 张智勇, 王方国, 邢光福, 郝国杰, 冯艳芳. 2009. 中国大地构造单元划分 [J]. 中国地质, 36(1): 1–28.
- 师淑娟, 王学求, 宫进忠. 2011. 金的地球化学异常与金矿床规模之间关系的统计学特征——以河北省为例 [J]. 中国地质, 38(6): 1562–1567.
- 宋相龙, 肖克炎, 丁建华, 范建福, 李楠. 2017. 全国重要固体矿产重点成矿区带数据集 [J]. 中国地质, 44(S1): 72–81.
- 孙启祯. 1994. 边缘成矿与成矿边缘效应 [J]. 地学前缘, (4): 176–183.
- 王登红. 2016. 对华南矿产资源深部探测若干问题的探讨——以若干超大型矿床深部找矿突破为例 [J]. 中国地质, 43(5): 1585–1598.
- 王来云, 孙念仁, 钟立平. 2010. 大兴安岭北段贵金属有色金属区域成矿地质特征及找矿方法 [J]. 吉林地质, 29(1): 36–40.
- 王磊, 胡兆国, 李向民, 闫海忠, 杨超. 2020. 甘肃省党河南山乌兰达坂沟—孔子沟地区水系沉积物地球化学特征及找矿远景预测 [J]. 中国地质, 47(2): 516–527.
- 王磊, 杨建国, 王小红, 齐琦, 李文明, 姜安定, 张洲远. 2016. 甘肃北山拾金坡—南金滩地区水系沉积物地球化学特征及找矿远景 [J]. 中国地质, 43(2): 585–593.
- 王新春, 齐钒宇, 李晓蕾, 高学正. 2016. 资料数据集成与服务研究——以整装勘查区地质工作为例 [J]. 中国地质, 43(2): 691–697.
- 王成辉, 王登红, 黄凡, 徐珏, 陈郑辉, 应立娟, 刘善宝. 2012. 中国金矿集区及其资源潜力探讨 [J]. 中国地质, 39(5): 1125–1142.
- 王杨刚, 李娜, 向运川, 刘国, 于艳, 张大可, 何翠云, 何学渊, 赵军, 吴文娟. 2015. 全球地质矿产数据建库方法技术研究 [J]. 中国地质, 42(1): 342–353.
- 汪东波, 江少卿, 董方浏. 2016. 藏北多龙矿集区荣那斑岩铜矿找矿突破的实践 [J]. 中国地质, 43(5): 1599–1612.
- 韦少港, 宋扬, 唐菊兴, 高轲, 冯军, 李彦波, 侯淋. 2016. 西藏色那铜(金)矿床石英闪长玢岩年代学、地球化学与岩石成因 [J]. 中国地质, 43(6): 1894–1912.
- 吴玉诗, 王海建, 车海龙, 赵虹旭, 马录录. 2020. 吉林省浑江市幅1:50 000水系沉积物测量原始数

- 据集 [DB/OL]. 地质科学数据出版系统. (2020-12-30). DOI: 10.35080/data.C.2020.P23.
- 奚小环, 李敏. 2012. 中国区域化探若干基本问题研究: 1999—2009[J]. 中国地质, 39(2): 267—282.
- 向运川, 牟绪赞, 任天祥, 刘荣梅, 吴轩. 2018. 全国区域化探数据库 [J]. 中国地质, 45(S1): 32—44.
- 杨剑, 唐发伟, 王桥, 王永华. 2015. 云南北衡地区成矿地球化学特征及找矿方向 [J]. 中国地质, 42(6): 1989—1999.
- 袁慧香, 王杨刚, 任永强, 王春女, 刘娜. 2015. 基于 ArcGIS 的整装勘查信息系统设计与建立 [J]. 中国地质, 42(1): 354—364.
- 赵武强, 崔森, 邹先武, 汤朝阳, 夏杰, 金世超. 2014. 湖南禾库地区水系沉积物地球化学特征及找矿预测 [J]. 中国地质, 41(2): 638—647.
- 张璟, 陈远荣, 谢桃园, 李凤友, 袁玉华, 赵俊, 宋御, 邹杰. 2010. 团结沟金矿床成因、构造控矿规律与找矿方向浅析 [J]. 中国地质, 37(6): 1710—1719.
- 张江华, 王葵颖, 赵阿宁, 陈华清, 柯海玲, 刘瑞平. 2013. 小秦岭金矿区水系沉积物重金属特征研究 [J]. 中国地质, 40(2): 602—611.
- 张万益, 聂凤军, 刘树文, 左力艳, 陕亮, 姚晓峰. 2013. 大兴安岭南段西坡金属矿床特征及成矿规律 [J]. 中国地质, 40(5): 1583—1599.
- 张永强, 谈乐, 李小明. 2019. 陕西石泉—旬阳金矿带整装勘查区饶峰幅等 7 个图幅区 1:50 000 水系沉积物测量原始数据集 [J]. 中国地质, 46(S1): 46—54.
- 张运强, 陈海燕, 张立国, 陈超, 刘应龙, 何娇月, 康璇, 张金龙, 彭芊芫. 2015. 冀北新杖子地区水系沉积物地球化学特征及找矿预测 [J]. 中国地质, 42(6): 1980—1988.
- 智云宝, 王增辉, 魏正宇, 赵西强. 2019. 1:50 000 山东毕郭幅地球化学数据集 [J]. 中国地质, 46(S1): 84—92.
- 朱炳玉, 杨隆勃, 朱亿广, 刘家军, 马华东. 2011. 新疆金山金矿床构造控矿规律及找矿评价标志研究 [J]. 中国地质, 38(1): 109—118.
- 左群超, 叶天竺, 冯艳芳. 2018. 中国陆域 1:25 万分幅建造构造图空间数据库 [J]. 中国地质, 45(S1): 1—26.

**doi: 10.12029/gc2020Z203**

Article Citation: Wu Yushi, Wang Haijian, Che Hailong, Zhao Hongxu, Ma Lulu, Li Aimin, Liu Chenchen, Sun Dongxue, Ma Ming, Li Dongyu. 2020. Primary Dataset of 1 : 50 000 Stream Sediment Survey of Hunjiang City Map-sheet, Jilin Province[J]. *Geology in China*, 47(S2):44–62.

Dataset Citation: Wu Yushi; Wang Haijian; Che Hailong; Zhao Hongxu; Ma Lulu. Primary Dataset of 1 : 50 000 Stream Sediment Survey of Hunjiang City Map-sheet, Jilin Province (V1). The Fourth Geological Survey of Jilin Province[producer], 2018. National Geological Archives of China[distributor], 2020-12-30. 10.35080/data.C.2020.P23; <http://dcc.cgs.gov.cn/en//geologicalData/details/doi/10.35080/data.C.2020.P23>.

Received: 06-05-2020

Accepted: 27-06-2020

**Fund Project:**

A subject project titled “Mineral Survey and Prospecting Predication of Integrated Exploration Area of Iron and Gold Deposits in Banshigou, Baishan City, Jilin Province” (Project No.: 121201004000 172201-06) of the China Geological Survey Project titled “Prospecting Predication and Technical Application Demonstration of Integrated Exploration Areas”

## Primary Dataset of 1 : 50 000 Stream Sediment Survey of Hunjiang City Map-sheet, Jilin Province

WU Yushi, WANG Haijian, CHE Hailong, ZHAO Hongxu, MA Lulu, LI Aimin,  
LIU Chenchen, SUN Dongxue, MA Ming, LI Dongyu

(The Fourth Geological Survey of Jilin Province, Tonghua 134001, Jilin, China)

**Abstract:** During the 1 : 50 000 stream sediment survey of Hunjiang City map-sheet, Jilin Province, a total of 1961 samples of stream sediments were collected, with the sample grain size ranging from -10 meshes to +80 meshes and average sampling density of 5.1 samples per km<sup>2</sup>. Sixteen elements, namely Au, Ag, Cu, Pb, Zn, As, Sb, Bi, Hg, W, Sn, Mo, Cd, Co, Cr and Ni, were analyzed using the techniques of atomic emission spectrometry (AES), adsorption of foam plastic by graphite furnace atomic absorption spectrometry (GFAAS), atomic fluorescence spectroscopy (AFS), and inductively coupled plasma mass spectrometry (ICP-MS), forming the primary dataset of 1 : 50 000 stream sediment survey of Hunjiang City map-sheet, Jilin Province (also referred to as the Dataset). The Dataset consists of one primary data table in Excel and a set of atlas in MapGIS format. The former is comprised of the primary analysis data of 16 elements for 1961 samples, and the later includes one mineral geological map, one sampling point bitmap, 16 single-element geochemical maps, and 16 single-element anomaly maps. On the basis of the Dataset, 403 single-element geochemical anomalies and 24 integrated anomalies were newly discovered. Meanwhile, three prospecting target areas of gold deposits and two of copper and polymetallic deposits were delineated based on the geological survey, geophysical and geochemical exploration, remote sensing data and existing metallogenic clues. The Dataset provides fundamental data for the map-sheet area and serves as a geochemical basis for geological research and applications in other fields.

**Key words:** geochemical data; stream sediment survey; dataset; mineral survey engineering; Hunjiang City; Jilin Province

**Data service system URL:** <http://dcc.cgs.gov.cn>

**About the first author:** WU Yushi, male, born in 1977, senior engineer, mainly engages in geological and mineral survey; E-mail: [593483266@qq.com](mailto:593483266@qq.com).

## 1 Introduction

The integrated exploration area of gold and iron deposits in Banshigou area, Baishan City, Jilin Province boasts rich mineral resources, mainly including Anshan-type iron deposits (Hong XW et al., 2010; Fu JF et al., 2014) and hydrothermal gold deposits (Zhu BY et al., 2011; Wang L et al., 2016) as well as copper, lead-zinc, magnesian dolomite, limestone and coal. More than 90% noble and nonferrous metal deposits in Jilin Province are distributed on the margins of geotectonic units and geologic blocks, showing the features of marginal mineralization (Sun QZ, 1994). The Jinying gold deposit, a large deposit recently discovered in the northern part of the Hunjiang City map-sheet, mainly occurs in the marble in the Zhenzhumen Formation that enjoys high Au abundance and on the contact zone between an ancient continent and the basal gravel-bearing sandstone of the formation (on the side close to continental margin). Therefore, it has developed at distinctive horizons. The Hunjiang City map-sheet area enjoys wide metallogenic geological space of Jinying-style gold deposits, large distribution area of regional metallogenic geologic blocks, and good consistency between geochemical anomalies with known ore-controlling structures (Chen BL et al., 2004), thus showing favorable geological conditions for metallogenesis and great prospecting potential. However, systematical, effective researches are yet to be carried out in this area in terms of ore-controlling factors, temporal-space distribution regularity, the evolutionary trajectory of geological history, and the regional metallogenic modes. The 1 : 200 000 stream sediment surveys involving this map-sheet were conducted during 1983–1986; however only part of anomalies were investigated and verified<sup>①</sup>. Therefore, the stream sediments were still at a low exploration level after these surveys. The 1 : 50 000 stream sediment survey of the metallogenic zones will help to figure out the geochemical distribution and concentration of main metallogenic elements in the survey area, narrow prospecting target areas, and verify crucial prospecting anomalies, thus providing basis for resource potential evaluation and basic geological research of mineralization (Li SM et al., 2009).

The 1 : 50 000 Hunjiang City map-sheet in Jilin Province is a proportion of Fe–Cu–Pb–Zn–Au–U–B–magnesite–talc–graphite–diamond metallogenic belt of Eastern Liaoning (uplift) (III–56) in the metallogenic province of North China (Block) (II–14) (Song XL et al., 2017), crossing the Sifangshan–Banshi iron prospecting area (V29) in the Fe–Au–Cu–Pb–Zn–gypsum metallogenic subzone of Tieling–Jingyu (secondary uplift) (III–56–①) and the Da'an Au–Fe–Cu–P prospecting area (V31) in the Pb–Zn–Fe–Au–Ag–U–B–magnesite–talc metallogenic sub-belt of Yingkou–Changbai (secondary uplift, Pt<sub>1</sub> rift) (III–56–②)<sup>②</sup> (Fig. 1).

The survey site experienced the formation of ancient blocks, the development of cover rocks and activities of continental margins, thus featuring complex geologic structures<sup>③</sup> (Pan GT et al., 2009; Liu X et al., 2015). Various Archean–Mesozoic strata are all exposed to varying extents in the survey site. Interfaces between different geological units and contact interfaces between different suite units tend to be tectonically weak and provide good pathways for hydrothermal activities of magma, serving as favourable metallogenic parts (Fig. 2; Wang

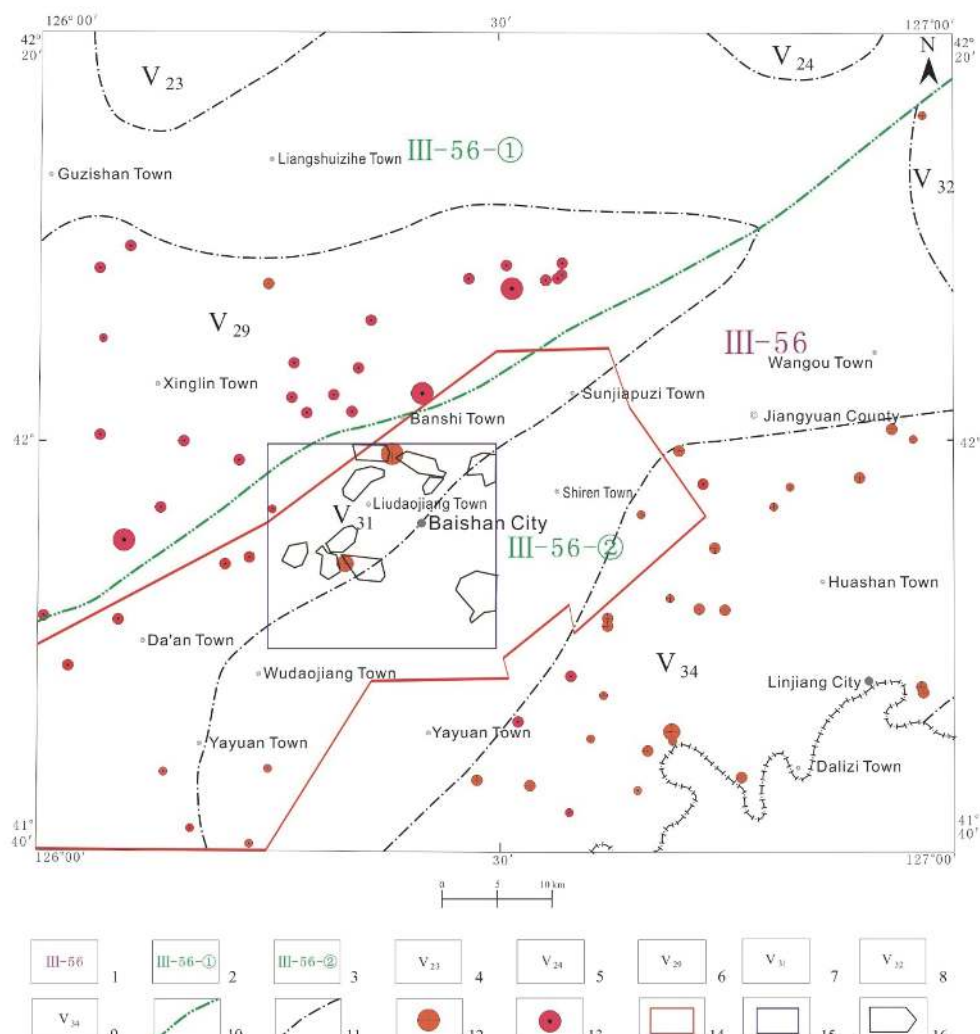


**Fig. 1 Location of metallogenic zones or belts covering the integrated exploration area of gold and iron deposits in Banshigou area, Baishan City, Jilin Province**

1—III-56: Fe—Cu—Pb—Zn—Au—U—B—magnesite—talc—graphite—diamond metallogenic belt of Eastern Liaoning (uplift); 2—III-56-①: Fe—Au—Cu—Pb—Zn—gypsum metallogenic subzone of Tieling—Jingyu (secondary uplift); 3—III-56-②: Pb—Zn—Fe—Au—Ag—U—B—magnesite—talc metallogenic subzone of Yingkou—Changbai (secondary uplift, Pt<sub>1</sub> rift); 4—V<sub>23</sub>: Huinan—Fumin Au—Fe prospecting area; 5—V<sub>24</sub>: Wangjiadian—Naerlong Au—Cu—Fe—Ni prospecting area; 6—V<sub>29</sub>: Sifangshan—Banshi Fe prospecting area; 7—V<sub>31</sub>: Da'an Au—Fe—Cu—P prospecting area; 8—V<sub>32</sub>: Fusong Pb—Zn prospecting area; 9—V<sub>34</sub>: Nancha—Huangoushan Au—Ag—Fe—Cu—Pb—Zn—S prospecting area; 10—Boundary of a grade IV metallogenic zone or belt; 11—Boundary of a grade V metallogenic zone or belt; 12—Gold deposit and ore occurrence; 13—Iron deposit and ore occurrence; 14—Range of the integrated exploration area of gold and iron deposits in Banshigou, Baishan City, Jilin Province; 15—Survey site of Hunjiang City map-sheet; 16—Delineation range of prospecting target area

LY et al., 2010; Zhang WY et al., 2013).

The project titled *Mineral Survey and Prospecting Predication of Integrated Exploration Area of Iron and Gold Deposits in Banshigou, Baishan City, Jilin Province* is a subject of the geological survey project titled *Prospecting Predication and Technical Application Demonstration of Integrated Exploration Areas* initiated by the China Geological Survey. It began in May 2018 and ended in December 2018, finishing 384 km<sup>2</sup> of 1 : 50 000 stream sediment survey and 384 km<sup>2</sup> of 1 : 50 000 mineral and geology-specific mapping, 364 km<sup>2</sup> of

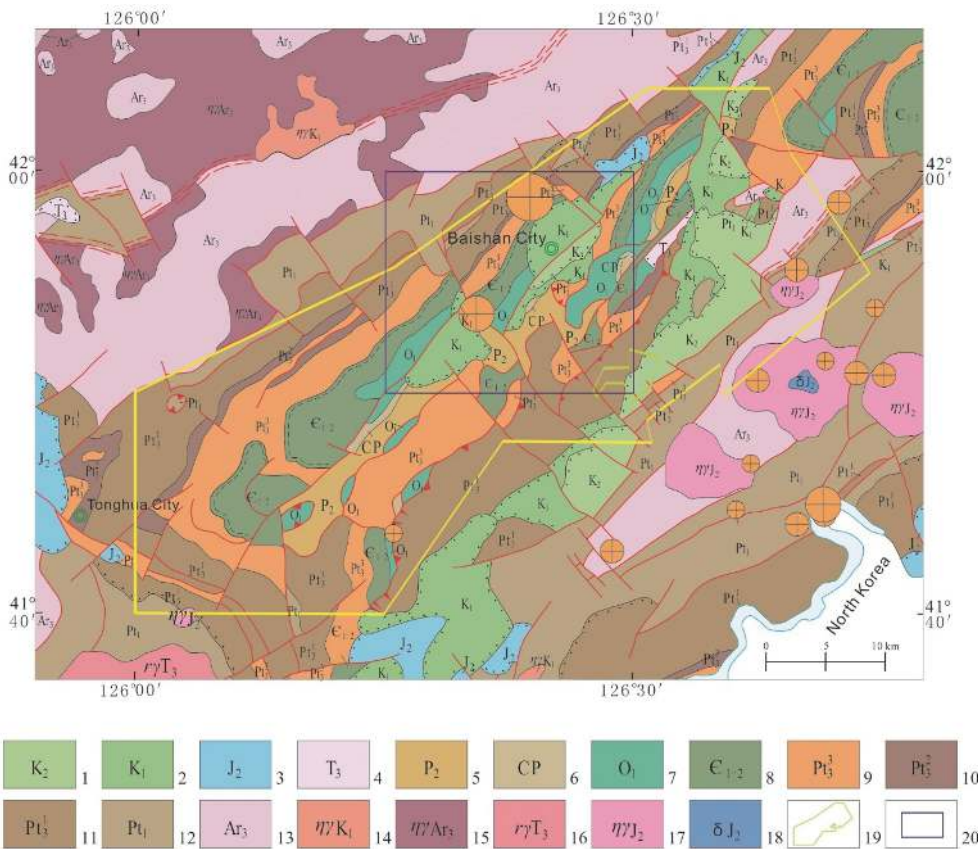


**Fig. 2 Geological map of the integrated exploration area of gold and iron deposits in Banshigou, Baishan City, Jilin Province**

1—Upper Cretaceous; 2—Lower Cretaceous; 3—Middle Jurassic; 4—Upper Triassic; 5—Middle Permian;  
6—Carboniferous—Permian; 7—Lower Ordovician; 8—Lower—Middle Cambrian; 9—Sinian; 10—Nanhuan System;  
11—Qiungbaikouan System; 12—Paleoproterozoic; 13—Neoarchean metamorphic supracrustal rock; 14—Early  
Cretaceous monzonitic granite; 15—Neoarchean monzonitic granite; 16—Late Triassic monzonitic granite; 17—Middle  
Jurassic monzonitic granite; 18—Middle Jurassic diorite; 19—Range of the integrated exploration area of gold and iron  
deposits in Banshigou, Baishan City, Jilin Province; 20—Survey site of the Hunjiang City map-sheet

1 : 50 000 high-precision magnetic survey, 384 km<sup>2</sup> of remote sensing and image interpretation, 200 m<sup>3</sup> of trenching, comprehensive inspections of two places, and tracing of one progress in the survey of the integrated exploration area. The Dataset (Wu YS et al., 2020; Table 1) was formed relying on the sub-project.

## 2 Methods for Data Acquisition and Processing

### 2.1 Selection of Methods

The survey site is situated in the Tonghua low-mid-mountainous forest landscape district (II<sub>3</sub>), which belongs to the hilly and low-mid-mountainous forest landscape subregion (II) in the middle part of Jilin Province, the forest-marsh landscape region of northeast China (I). It features the climate of humid and rainy summer and autumn, strong denudation, and deep cutting, with physical weathering prevailing, thus suitable for stream sediment survey (Xi XH et al., 2012). According to the *Specification of Geochemical Reconnaissance Survey (1 : 50 000)* (DZ/T0011- 2015; also referred to as the *Specification*) and the features of the

**Table 1 Metadata Table of Database (Dataset)**

| Item                           | Description   |
|--------------------------------|---|
| Database (dataset) name        | Primary Dataset of 1 : 50 000 Stream Sediment Survey of Hunjiang City Map-sheet, Jilin Province   |
| Database (dataset) authors     | Wu Yushi, The Fourth Geological Survey of Jilin Province<br>Wang Haijian, The Fourth Geological Survey of Jilin Province<br>Che Hailong, The Fourth Geological Survey of Jilin Province<br>Zhao Hongxu, The Fourth Geological Survey of Jilin Province<br>Ma Lulu, The Fourth Geological Survey of Jilin Province   |
| Data acquisition time          | From May 2018 to December 2018  |
| Geographical area              | 1 : 50 000 Hunjiang City map-sheet, Jilin Province lies in the southeastern part of Jilin Province and in the middle part of the integrated exploration area of iron and gold deposits in Banshigou, Baishan City, Jilin Province, covering an area of 384 km <sup>2</sup> ; Coordinates: 126°15'00"-126°30'00"E; 41°50'00"-42°00'00"N  |
| Data formats                   | *.xlsx, *.wt, *.wl, *.wp  |
| Data size                      | 75.7 MB   |
| Data service system URL        | <a href="http://dcc.cgs.gov.cn">http://dcc.cgs.gov.cn</a>   |
| Fund project                   | The project titled <i>Mineral Survey and Prospecting Predication of Integrated Exploration Area of Iron and Gold Deposits in Banshigou, Baishan City, Jilin Province</i> (No.: 121201004000172201-06), which is a subject of the geological survey project titled <i>Prospecting Predication and Technical Application Demonstration of Integrated Exploration Areas</i> (No.: 121201004000172201) initiated by the China Geological Survey |
| Language                       | Chinese   |
| Database (dataset) composition | The Dataset consists of one data table in Excel and a set of atlas in MapGIS format. The former is composed of the primary analysis data of 16 elements for 1961 samples, and the later includes one mineral geological map, one sampling point bitmap, 16 single-element geochemical maps and 16 single-element anomaly maps   |

geochemical landscapes in the survey site, stream sediments were mainly sampled in this geochemical reconnaissance, with sampling density of 4–8 points per km<sup>2</sup> and sample grain size of –10 to +80 meshes. The sampling points were deployed at the estuary of first-order streams and within second-order streams, while control points were appropriately arranged in third-order streams.

## 2.2 Sampling Density

The sampling density was designed to be four points per km<sup>2</sup> in minor survey areas, 6–8 points per km<sup>2</sup> in key metallogenic zones/belts, and 1–2 points per km<sup>2</sup> in the areas with no stream developing such as valley terraces, piedmont plains, and eolian deposit areas. A total of 1961 samples of stream sediments were collected, with average sampling density of 5.1 samples per km<sup>2</sup>.

## 2.3 Sampling

### 2.3.1 Determination of Field Sampling Points

The sampling points of stream sediments were arranged according to the 1 : 50 000

topographic map of a standard map-sheet (the base map) with a projection type of Gauss–Kruger (transverse elliptic cylinder equiangular) projection and ellipsoid parameters of National Geodetic Coordinate System 2000 (CGCS 2000). Then the sampling points in the field were determined by using the digital mapping system (DGSS) installed in the palm-sized personal digital assistants (PDAs) of series UG-9 and the topographic map (Li CL et al., 2002; Guo FS et al., 2012). Before sampling, each of the PDAs was calibrated based on the reference points issued by the Jilin Bureau of Surveying, Mapping and Geoinformation. The errors of actual distances of all sampling points were less than 30 m, i.e. less than 0.6 mm on the freehand map, meeting the requirement that the errors in the field spotting should be less than 50 m as specified in the *Specification*.

### 2.3.2 Sampling Positions

In the areas with streams developing, samples were taken from the bottom of streams and valleys or the positions where alluviums of various grain sizes converge, such as locations where water flow slows down or stagnates, the inner side of the position where a channel is diverted, and places behind large rocks. (Zhang YQ et al., 2019). In the areas where feather-shaped streams are distributed, samples were acquired by combing the materials taken from multiple parallel streams within a sampling cell. In the troughs or channels that are dry or have intermittent water flow, fine-grained materials were collected at the bottom of riverbed to exclude the disturbance of eolian materials.

When sampling in small streams or piedmont streams without any apparent or typical surface runoff, samples were effectively taken along runoff direction from larger streams.

In the areas where no stream develops (including weathering areas of granite and landscape areas with apparent concave landform), water flow was determined according to the central line of the concave landform. Then along the two sides centering on the water flow, 3–5 soil samples were equidistantly taken from the surfaces with negative relief and wide gentle transverse sections (Zhi YB et al., 2019).

All samples were taken at designed positions and local adjustment did not affect the control scope of the samples. Meanwhile, all points added, abandoned, or changed were recorded.

### 2.3.3 Sample Materials

In the areas where streams develop, sampling materials mainly included mid-coarse grained sandstone and detritus in alluvium and diluvium. To make each sample more representative, each sample was taken from multiple (3–5) positions within 30 m around a sampling point.

In the areas where no stream develops, each sample was taken from multiple positions of soils instead of streams. Specifically, the samples were taken from the eluvial materials between B and C horizons of soils, and sample materials were the bedrock substances that can represent the original geological prospecting information in principle.

The original samples taken in the field were more than 500 g, and the final samples sieved were equal to or greater than 300 g, meeting the requirement that both the samples to be

transformed for testing and the samples to be reserved as duplicate samples should be greater than 150 g.

#### 2.4 Sample Processing

The samples were generally processed as follows: natural-air drying → kneading evenly or cracking → sieving → mixing evenly → weighing → bagging → boxing up → transporting for testing.

① The samples were air dried, during which they were frequently kneaded and cracked with a stick to avoid caking. In rainy seasons, special attentions should be paid to prevent loss or contamination of the samples caused by rain, wind-blown sand, or human factors.

② The fully dried samples were sieved with a nest of stainless-steel sieves of -10 meshes and +80 meshes. As a result, more than 300 g of samples were obtained after discarding the samples remaining on the top sieve and passing through the sieves.

③ The samples obtained were separated by quartering method. Afterwards, 150 g of samples were encapsulated with kraft bag for analysis and testing, and the remaining 150 g of samples were boxed up and reserved as duplicate samples.

#### 2.5 Methods for Sample Analysis and Testing

In strict accordance with the *Supplemental Technical Regulation on Sample Analysis of the Specification of Geochemical Reconnaissance Survey* issued by China Geological Survey in 2007, the samples were tested and analyzed in Liaoning Testing Institute under the China National Geological Exploration Center of Building Materials Industry, which holds a level-A qualification of rock and mineral testing.

According to project contracts and annual design requirements, the 1 : 50 000 stream sediment survey focused on the analysis of 16 elements, namely Au, Ag, Cu, Pb, Zn, As, Sb, Bi, Hg, W, Sn, Mo, Cd, Co, Cr, and Ni (Zhang JH et al., 2013; Zhao WQ et al., 2014).

The analysis scheme consisting of various analysis methods and testing means dominated by ICP-MS (Table 2) was developed based on optimization, selection, and study. The required detection limits of analysis and method detection limits meet the requirements of analysis and testing quality of stream sediment elements (Table 3).

#### 2.6 Data Processing

Data were processed using Geochem Studio 3.5.3, an integrated software system of geochemical exploration that was independently developed by the Institute of Geophysical and Geochemical Exploration, Chinese Academy of Geological Sciences. After gridding of discrete

**Table 2 Analysis methods and scheme**

| Analysis method   | Elements tested                               | Testing accuracy |
|---|---|------------------|
| Atomic emission spectrometry (AES)                      | Ag  | ≥ 0.01 nm        |
| Graphite furnace atomic absorption spectrometry (GFAAS) | Au  | ≥ 0.002 nm       |
| Atomic fluorescence spectroscopy (AFS)                  | As, Hg  | ≥ 0.3 nm         |
| Inductively coupled plasma mass spectrometry (ICP-MS)   | Cr, Co, Ni, Cu, Zn, Mo, Cd, Sn, Sb, W, Pb, Bi | 0.01–10 µg/L     |

**Table 3 Comparison between required detection limits of analysis and method detection limits**

| No. | Elements | Method detection limit | Required detection limit | Unit             | Analysis method |
|-----|----------|------------------------|--------------------------|------------------|-----------------|
| 1   | Cr       | 10                     | 15                       | $\times 10^{-6}$ | ICP-MS          |
| 2   | Co       | 0.5                    | 1                        | $\times 10^{-6}$ | ICP-MS          |
| 3   | Ni       | 2                      | 3                        | $\times 10^{-6}$ | ICP-MS          |
| 4   | Cu       | 1                      | 1.5                      | $\times 10^{-6}$ | ICP-MS          |
| 5   | Zn       | 5                      | 15                       | $\times 10^{-6}$ | ICP-MS          |
| 6   | Mo       | 0.2                    | 0.5                      | $\times 10^{-6}$ | ICP-MS          |
| 7   | Cd       | 0.1                    | 0.1                      | $\times 10^{-6}$ | ICP-MS          |
| 8   | Sn       | 0.5                    | 1                        | $\times 10^{-6}$ | ICP-MS          |
| 9   | Sb       | 0.03                   | 0.2                      | $\times 10^{-6}$ | ICP-MS          |
| 10  | W        | 0.2                    | 0.5                      | $\times 10^{-6}$ | ICP-MS          |
| 11  | Pb       | 2                      | 5                        | $\times 10^{-6}$ | ICP-MS          |
| 12  | Bi       | 0.1                    | 0.1                      | $\times 10^{-6}$ | ICP-MS          |
| 13  | As       | 0.5                    | 1                        | $\times 10^{-6}$ | AFS             |
| 14  | Hg       | 0.005                  | 0.0005                   | $\times 10^{-6}$ | AFS             |
| 15  | Ag       | 0.02                   | 0.03                     | $\times 10^{-6}$ | AES             |
| 16  | Au       | 0.0003                 | 0.0003                   | $\times 10^{-6}$ | GFAAS           |

data (grid spacing: 300 m × 300 m), the data lying outside 3 standard deviations (3S) of the mean in the normal distribution were gradually eliminated (Wang XC et al., 2016).

### 2.6.1 Data Processing Flow

#### (1) Inspection of data distribution pattern

According to the law of large numbers in statistics, an element tends to be distributed in a normal distribution pattern in case of enough samples. After Skewness and Kurtosis verification using the data (whereby the data lying outside 3S of the mean had been eliminated), all 16 elements tended to be distributed in arithmetic normal distribution pattern. Therefore, the arithmetic mean method was used to determine the mean and deviation.

#### (2) Statistical calculation of geochemical parameters

The background dataset was obtained based on the primary dataset of the 16 elements in the map-sheet as follows (Liu H et al., 2015): (1) conducting gridding of discrete data (grid spacing: 300 m × 300 m); (2) determining anomaly threshold through gradual elimination of data; (3) repeatedly eliminating data lying outside 3S of the mean in the normal distribution until no data can be eliminated. The threshold ( $T$ ) was calculated based on the mean of all the data ( $\bar{X}$ ) and the standard deviation ( $S$ ) according to the formula  $T=\bar{X}+1.65S$ . In this way, the anomaly threshold was finally determined.

#### (3) Setting of the parameters for mapping

With the inverse distance weighted (IDW) interpolation method, the data of sampling points were converted into the data available on a regular (rectangular) grid that are used to prepare geochemical maps. Relevant parameters were set as follows: distance power: 2; search directions: four-way search; data point number in each way: 6; minimum effective data point

number in each way: 5; permitted maximum number of ways without effective data: 4; grid spacing: 300 m × 300 m, and search radius: 2000 m.

A total of 1961 samples were collected in the 1 : 50 000 stream sediment survey, including 101 soil samples. These soil samples are sporadically distributed in the sampling cells and their grain sizes are consistent with those of the stream sediment samples, thus exposing no effect on the results of data processing.

## 2.6.2 Map Preparation

### (1) Draft data maps

Draft data maps mainly include streams, main residential areas, main surface feature indicators, roads, kilometer grids with Gauss-Kruger projection, latitudes and longitudes, locations of sampling points, and sampling information. Repeated sampling points and quality inspection points were marked with different colors or symbols.

### (2) Geochemical maps of elements

The isoline color zones were presented by the 15-level color gradation method, as specified in the *Geochemical Survey Specification*(1 : 50 000) (DZ/T0011- 2015). The isolines were plotted using corresponding content interval. Meanwhile, the intervals between different isolines of various color grades and levels were expressed with transitional color levels, in order to achieve the gradual change effect of relevant zones or belts in the same color level.

### (3) Geochemical anomaly maps

The survey site was divided into two zones according to the background distribution of the geochemical maps, geologic blocks, and tectonics. In details, the geochemical zones were determined according to the interrelations between geochemical maps and the geologic blocks in the geological maps. Afterwards, geochemical anomalies were straightly delineated after contrast values were calculated using the anomaly thresholds of the zones.

### (4) Composite anomaly maps

Based on the single-element anomaly maps, R-type cluster analysis and factor analysis were carried out on the primary data of the survey site using the software Geochem Studio 3.5.3. After that, the characteristics of element associations were determined using the analytical results. Then 3–5 elements were selected to prepare the isolines (anomaly lines). Meanwhile, a major element was identified to plot the values of gradation as well as the graded isolines and equivalence regions of anomaly concentration. The isolines were presented with lines of different colors as specified by the specification. For the equivalence regions, different surface colors were used to represent the inner, middle, and outer zones of anomalies.

### (5) Metallogenic prediction maps

Based on the analysis of various geochemical maps, prospecting areas and prospecting target areas were determined according to geological significance, classification and evaluation results of geochemical anomalies, geochemical anomaly associations and their spacious distribution regularity, and geological conditions.

### 3 Description of Data Samples

The Dataset consists of one geochemical analysis data table and maps in MapGIS format. The data types of element geochemical analysis data are character and floating point (Xiang YC et al., 2018; Table 4). The maps include draft data maps, geochemical maps of elements, geochemical anomaly maps, integrated anomaly maps and metallogenic prediction maps. They are comprised of point, line and polygon files in MapGIS format. The data types of the data in MapGIS format are long, double, character and floating point (Table 5, Table 6, Table 7). Attribute structures of all elements analyzed and the attribute structures of the point, line and polygon files in the maps were established according to the contents and structures of the solid mineral exploration databases adopted by the China Geological Survey (Li CL et al., 2013; Zuo QC et al., 2018), and the data structures (Wang YG et al., 2015; Yuan HX et al., 2015) were filled in completely.

### 4 Data Quality Control and Assessment

As mentioned above, the Liaoning Testing Institute under the China National Geological Exploration Center of Building Materials Industry selected analysis methods and detection limits according to the elements to be analyzed. Both the accuracy and precision of the analysis methods met the requirements specified in the *Specification*. The detection limits and reported rates of all elements are listed in Table 8.

In terms of quality management, internal and external quality monitoring were adopted together, with the external quality monitoring prevailing. As required by the China Geological Survey, the standard samples for external quality monitoring were purchased from the Institute of Geophysical and Geochemical Exploration, Chinese Academy of Geological Sciences. For the external quality monitoring, 100 standard samples were inserted at a proportion of 5% to total sample number. For internal quality monitoring, four control samples were inserted into every 50 samples (one analysis group), and 12 primary reference materials of soil were inserted in every 500 samples. Analysis methods were monitored in terms of accuracy, precision,

**Table 4 Geochemical analysis data table of elements of Hunjiang City Map-sheet**

| Serial number | Field name                   | Data type      | Example      | Serial number | Field name | Data type      | Example |
|---------------|------------------------------|----------------|--------------|---------------|------------|----------------|---------|
| 1             | Analysis batch character no. | character      | 2018 Hua 302 | 11            | Bi         | floating point | 0.25    |
| 3             | Mineral sample no.           | character      | HJS001C1     | 12            | Hg         | floating point | 0.034   |
| 4             | Au                           | floating point | 1.00         | 13            | W          | floating point | 1.41    |
| 5             | Ag                           | floating point | 70.80        | 14            | Sn         | floating point | 2.30    |
| 6             | Cu                           | floating point | 16.40        | 15            | Mo         | floating point | 0.84    |
| 7             | Pb                           | floating point | 19.40        | 16            | Cd         | floating point | 0.09    |
| 8             | Zn                           | floating point | 88.10        | 17            | Co         | floating point | 14.60   |
| 9             | As                           | floating point | 6.44         | 18            | Cr         | floating point | 71.20   |
| 10            | Sb                           | floating point | 0.57         | 19            | Ni         | floating point | 27.00   |

Notes: the content unit of Au and Hg is  $\times 10^{-9}$ , and that of other elements is  $\times 10^{-6}$ .

**Table 5 Metadata features and types of points in element geochemical maps of Hunjiang City Map-sheet**

| No. | Field name              | Data types       | Example                   |
|-----|-------------------------|------------------|---------------------------|
| 1   | ID                      | long integer     | 1                         |
| 2   | Anomaly no.             | character        | Ag-1                      |
| 3   | Location                | character        | (292 208.88, 4653 922.84) |
| 4   | Anomaly point number    | long integer     | 3                         |
| 5   | Threshold of anomaly    | double precision | 1                         |
| 6   | Anomaly area            | double precision | 0.558 407                 |
| 7   | Ordinal of anomaly area | long integer     | 7                         |
| 8   | Mean                    | double precision | 1.143 667                 |
| 9   | Ordinal of mean         | long integer     | 12                        |
| 10  | Maximum                 | double precision | 1.231                     |
| 11  | Ordinal of maximum      | long integer     | 12                        |
| 12  | Contrast                | double precision | 1.143 667                 |
| 13  | Ordinal of contrast     | long integer     | 12                        |
| 14  | AD                      |                  | 0.638 632                 |
| 15  | Ordinal of AD           | long integer     | 8                         |
| 16  | AP                      | double precision | 0.080 224                 |
| 17  | Ordinal of AP           | long integer     | 11                        |
| 18  | NAD                     | double precision | 0.638 632                 |
| 19  | Ordinal of NAD          | long integer     | 8                         |
| 20  | NAP                     | double precision | 0.080 224                 |
| 21  | Ordinal of NAP          | long integer     | 8                         |
| 22  | Number of belts         | long integer     | 1                         |

**Table 6 Metadata features and types of lines in element geochemical maps of Hunjiang City Map-sheet**

| Serial number | Field name  | Data type        | Example    |
|---------------|-------------|------------------|------------|
| 1             | ID          | long integer     | 1          |
| 2             | Length      | double precision | 80.556 64  |
| 3             | Height      | double precision | 1          |
| 4             | Element no. | character        | Ag-1       |
| 5             | bh          | character        | Ag-1       |
| 6             | UserID      | long integer     | -1         |
| 7             | MAPCODE     | character        | K52E013002 |
| 8             | CHFCAC      | character        | 1          |
| 9             | YSY CZ      | floating point   | 0.12       |
| 10            | YSY CLX     | character        | 0          |
| 11            | YCTZ        | character        | 0          |
| 12            | YCDZ        | floating point   | 0.15       |
| 13            | HLZ         | floating point   | 0.08       |

**Table 7 Metadata features and types of polygons in element geochemical maps of Hunjiang City Map-sheet**

| Serial number | Field name  | Data type        | Example    |
|---------------|-------------|------------------|------------|
| 1             | ID          | long integer     | 16         |
| 2             | Area        | double precision | 433.29     |
| 3             | Perimeter   | double precision | 271.77     |
| 4             | MAPCODE     | character        | K52E013002 |
| 5             | Start_value | double precision | 1          |
| 6             | end_value   | double precision | 2          |

**Table 8 Detection limits and reported rates of analysis methods**

| Serial number | Element detected | Detection limit of analysis method | Detection limit required in the <i>Specification</i> | Reported rate/% | Analysis method |
|---------------|------------------|------------------------------------|--|-----------------|-----------------|
| 1             | Au               | 0.0003                             | 0.0003   | 100             | GFAAS           |
| 2             | Ag               | 0.02                               | 0.03   | 100             | AES             |
| 3             | Cu               | 1.0                                | 1.5  | 100             | ICP-MS          |
| 4             | Pb               | 2                                  | 5  | 100             | ICP-MS          |
| 5             | Zn               | 5                                  | 15   | 100             | ICP-MS          |
| 6             | As               | 0.5                                | 1  | 100             | AFS             |
| 7             | Sb               | 0.03                               | 0.2  | 100             | ICP-MS          |
| 8             | Bi               | 0.1                                | 0.1  | 100             | ICP-MS          |
| 9             | Hg               | 0.005                              | 0.0005   | 100             | AFS             |
| 10            | W                | 0.2                                | 0.5  | 100             | ICP-MS          |
| 11            | Sn               | 0.5                                | 1  | 100             | ICP-MS          |
| 12            | Mo               | 0.2                                | 0.5  | 100             | ICP-MS          |
| 13            | Cd               | 0.1                                | 0.1  | 100             | ICP-MS          |
| 14            | Co               | 0.5                                | 1  | 100             | ICP-MS          |
| 15            | Cr               | 10                                 | 15   | 100             | ICP-MS          |
| 16            | Ni               | 2                                  | 3  | 100             | ICP-MS          |

Notes: inductively coupled plasma mass spectrometry (ICP-MS), atomic fluorescence spectroscopy (AFS) and adsorption of foam plastic by graphite furnace atomic absorption spectrometry (GFAAS)

systemic errors, and accidental errors. As a result, the element accuracy was 100% and the precision met the requirements in the specification.

Internal inspection and quality monitoring of anomalous points: internal inspection and analysis were conducted on 8% of all samples, and spot check for anomalies was performed on some samples with high or low element content. For the quality monitoring of the internal inspection and anomaly spot check of each element, statistics were made for qualification rates based on relative deviation  $RD \leq 25\%$ . As a result, the first-time qualification rate was  $\geq 90\%$ .

To avoid geochemical pseudomorph caused by the analysis of accidental errors, the mutant high- and low-values in some analytical results were repeatedly inspected after the analysis of each batch of samples. Spot check was conducted on a total of 1824 items of anomalous points, accounting for 6.13% of all items. As a result, 1 799 items were qualified,

with an overall qualification rate of 98.63%.

Internal inspection and spot check of anomalous points were conducted on a total of 3 008 items, accounting for 10.09%. As a result, 2 962 items were qualified, with an overall qualification rate of 98.47%.

For various sample analysis data, the analysis report and data disk were provided by analytical organization. They were checked and confirmed by data processing staff, and then put in storage. They can be used only after being guaranteed to be correct through multiple verifications. After checking calculations with a set of standard data, various calculations were performed using corresponding calculation programs. The preparation of maps and data tables and the citation of various data were all checked, ensuring that all data were collated correctly and accurately.

## 5 Delineation and Features of Anomalies

### (1) Delineation of Anomalies

Single-element anomalies were directly delineated in computers based on the anomaly threshold of geochemical zones. Integrated anomalies were determined by manual intervention based on the single-element anomalies delineated, during which anomalies were broken down or properly adjusted according to geological background, features of anomaly element associations, and landform and topographic factors and some small single-point anomalies were deleted (Li SM et al., 2014).

Major and associated metallogenic elements in the map-sheet were determined according to the anomaly scales (NAP) of various elements in the integrated anomalies of the 16 major metallogenic elements (Shi SJ et al., 2011). In detail, they mainly depended on elements that ranked top among single-element anomalies throughout the area for their scales and had the largest single-element anomaly scale in integrated anomalies.

A total of 403 single-element anomalies and 24 integrated anomalies were delineated, with nos. from Hunhun 18HS-1 to 18HS-24. They were registered, interpreted and ranked. As a result, a total of three anomalies of class A<sub>1</sub>, seven anomalies of Class-B<sub>2</sub>, and 14 anomalies of Class-B<sub>3</sub> were determined (Table 9).

The Banmiaozi gold deposit (Jinying gold deposit) is distributed in the anomalous area of Hunhun 18HS-2. As is one of the important large concealed gold deposits in Baishan area, Jilin Province, it is regionally representative and has great resource potential (Wang DH, 2016). No apparent 1 : 200 000 geochemical anomalies are available in this deposit. The main indicator elements of geochemical exploration (Wang L et al., 2020) determined in this 1 : 50 000 stream sediment survey mainly include Au, Cu, As, Hg, and Cd. Among these elements, As is generally located in the anomaly inner zones, Hg and Cu in mesozones and outer zones of anomalies, and Au and Cd mostly in mesozones and outer zones of anomalies. Meanwhile, As, Sb, Hg and V are the front halo elements of mineral bodies (Niu SY et al., 2012) and can serve as the prospecting indicators of concealed gold deposits. More than 60 km<sup>2</sup> of metallogenic geologic blocks similar to Banmiaozi Gold deposit are distributed in the northwestern part of

**Table 9 Features of integrated anomalies of major metallogenic elements<sup>a</sup>**

| Anomaly no.   | Element association<br>(descending order by scale)<br>(NAP) | Scale<br>(NAP) | Major and associated metallogenic<br>elements (scale)  | Anomaly<br>class |
|---------------|---|----------------|--|------------------|
| Hunhun18HS-1  | Cd–As–Hg–Au–Bi  | 7.28           | Cd(3.67)   | B <sub>3</sub>   |
| Hunhun18HS-2  | Au–Cr–Hg–As–Cd–Cu–Ni  | 34.20          | Au(22.81) Cr(4.12)   | A <sub>1</sub>   |
| Hunhun18HS-3  | Au–Cr–Hg  | 13.1           | Au(7.85) Cr(4.77)  | B <sub>3</sub>   |
| Hunhun18HS-4  | As–Hg–Sb–Cr–Mo–W–Ni–Ag–Co–Sn–Cu                             | 47.76          | Sb(10.69) Cr(5.35) Mo(3.52) W(1.48) Ni(1.41) Ag(1.12) Co(1.03)                                     | B <sub>2</sub>   |
| Hunhun18HS-5  | Cr–Au–Cu–Ni–Sb–Mo–W   | 33.32          | Cr(13.69) Au(6.75) Cu(4.41) Ni(3.55) Sb(2.57) Mo(1.64)   | B <sub>2</sub>   |
| Hunhun18HS-6  | Hg–Sb–Au–W–Mo–Cd–As–Pb                                      | 36.77          | Sb(9.45) Au(5.38) W(2.24) Mo(1.96) Cd(1.50)  | B <sub>2</sub>   |
| Hunhun18HS-7  | Cr–Mo–Cu–Ni–As–Sb   | 8.04           | Cr(2.65) Mo(2.23) Cu(2.13) Ni(1.49)  | B <sub>3</sub>   |
| Hunhun18HS-8  | Au–Sb–Cr–Hg–W–Cu–As–Mo                                      | 48.54          | Au(19.96) Sb(11.73) Cr(7.34) W(2.38)   | B <sub>2</sub>   |
| Hunhun18HS-9  | W–Cr–Au–Sb  | 7.68           | W(2.69) Cr(2.60) Au(1.75)  | B <sub>3</sub>   |
| Hunhun18HS-10 | Cr–As–Sb–Bi–Cu–Zn–Pb–Co–Mo–Au–Ni–Sn–Cd                      | 41.59          | Cr(12.4) Sb(4.11) Bi(3.24) Cu(2.33) Zn(2.23) Pb(1.75) Co(1.63) Mo(1.43) Au(1.36)                   | B <sub>3</sub>   |
| Hunhun18HS-11 | Sb–Mo–W–As–Hg–Cu–Ni   | 6.49           | Sb(1.38) Mo(1.05) W(1.03)  | B <sub>3</sub>   |
| Hunhun18HS-12 | Co–Cr–Mo–Cu–Pb–Sn–Au–Ni–Bi                                  | 22.74          | Co(10.21) Cr(3.37) Mo(3.30) Cu(2.32) Pb(1.37)  | B <sub>3</sub>   |
| Hunhun18HS-13 | Mo–Au–Cu–W–Cd–Sb–Cr–Hg                                      | 44.54          | Mo(12.72) Au(7.39) Cu(6.98) W(5.75) Cd(3.92) Sb(3.42) Cr(3.21)                                     | B <sub>2</sub>   |
| Hunhun18HS-14 | Cr–Sb–Mo–Ni–As–Cu–Co–Ag–Cd                                  | 23.19          | Cr(8.35) Sb(5.19) Mo(2.70) Ni(2.26)  | B <sub>3</sub>   |
| Hunhun18HS-15 | Au–Cr–Ag–Cu–Cd–Pb–Bi–Sb–Zn–As–W–Co                          | 26.89          | Au(7.23) Cr(4.17) Ag(3.57) Cu(2.80) Cd(2.60) Pb(2.01) Bi(1.21) Sb(1.10)                            | B <sub>2</sub>   |
| Hunhun18HS-16 | Au–Ag–Cu–Cr–Cd–Bi–Zn–Pb–Mo–As–Sb–W                          | 90.87          | Au(41.68) Ag(9.37) Cu(6.68) Cr(6.20) Cd(6.05) Bi(4.54) Zn(4.53) Pb(4.46) Mo(3.03) Sb(1.17) W(1.00) | A <sub>1</sub>   |
| Hunhun18HS-17 | Au–Ag–Cu–Mo–Sb–Hg–As–Cr–Pb–W–Cd–Ni–Sn                       | 80.04          | Au(41.68) Ag(6.87) Cu(5.57) Mo(5.40) Sb(5.30) Cr(3.41) Pb(2.01) W(1.42)                            | A <sub>1</sub>   |
| Hunhun18HS-18 | Sb–As–Au–Cd–W–Co–Cu   | 12.04          | Sb(3.37) Au(2.20) Cd(1.61) W(1.14)   | B <sub>3</sub>   |
| Hunhun18HS-19 | Cr–Au–Cu–Sn–Hg–Bi   | 13.59          | Cr(5.70) Au(2.99) Cu(2.88) Sn(1.08)  | B <sub>3</sub>   |
| Hunhun18HS-20 | As–Sb–Co–Cr–Au–Ag–Cu–Pb–Cd–Ni–Zn–Hg–Sn–W                    | 55.60          | Sb(7.41) Co(6.81) Cr(5.79) Au(5.60) Ag(4.32) Cu(3.76) Pb(3.41) Cd(2.84) Ni(2.59) Zn(2.20)          | B <sub>2</sub>   |
| Hunhun18HS-21 | Cr–Cu–Ag–Co–Ni–Hg–Pb–Sn–Bi                                  | 24.87          | Cr(6.95) Cu(4.66) Ag(3.47) Co(3.41) Ni(2.66)   | B <sub>3</sub>   |
| Hunhun18HS-22 | W–Hg–Cr–Mo–Au–Bi–As–Sn–Zn–Cu–Pb                             | 13.71          | W(3.28) Cr(2.13) Mo(1.27)  | B <sub>3</sub>   |
| Hunhun18HS-23 | Pb–As–Cd–Hg–Mo–Cu–Ni  | 8.75           | Pb(2.18) Cd(1.90)  | B <sub>3</sub>   |
| Hunhun18HS-24 | Hg–Sb–Cr–Cd–Cu–Pb–Bi–W–Ni–Co                                | 25.83          | Sb(5.32) Cr(4.05) Cd(3.77) Cu(1.75) Pb(1.20)   | B <sub>3</sub>   |

the map-sheet and their anomalies overlap well, providing sufficient geological space for breakthroughs in prospecting of such gold deposits. Furthermore, Liujiapuzi–Langdonggou

Gold–Silver Deposit is distributed in the range of Hunhun 18HS-16. The main indicator elements of geochemical exploration in the deposit include Au, Ag, Cu, Pb, Cd, As, Sb, Hg, W, Mo, and Bi. Among these elements, Sn, W, As, and Sb are generally located in the inner zones, Cd and Bi in the mesozones, and Cu, Mo, and Au (and Ag) in the outer zones. Cu-bearing granodiorite-porphyry was discovered through anomaly check. This indicates the prospecting potential of porphyritic copper-gold deposits (Wei SG et al., 2016) and serves as a significant factor for further prospecting. Multiple integrated anomalies similar to Hunhun 18HS-2, and Hunhun 18HS-16 are distributed in the map-sheet, and they enjoy super metallogenic geological conditions (Zhang YQ et al., 2015; Yang J et al., 2015). All these provide favorable conditions for making breakthroughs in prospecting of epithermal gold and polymetallic deposits (Zhang J et al., 2010; Wang CH et al., 2012) and porphyritic copper (gold) deposits (Wang DB et al., 2016) in the integrated exploration area.

Through anomaly inspection, mineralized altered bodies or anomalous geologic blocks were found in anomalies of classes A<sub>1</sub> and B<sub>2</sub>. Furthermore, the Jinying Gold Deposit and Liujiapuzi–Langdonggou Gold–Silver Deposit in Baishan City, Jilin Province were discovered in the anomalies of class A<sub>1</sub>. All these demonstrate that the ranking, assessment, and classification of the anomalies mentioned above were accurate.

#### (2) General features of the anomalies

The geochemical anomalies are distributed regularly to some extent. In general, they are mostly in NE trending and are significantly controlled by the strike of the strata in the northwestern wing of Hunjiang Syncline. Additionally, they are in NW or nearly WE trending locally. Besides, the distribution of the anomalies tends to relate to fault structures to a certain degree. Geochemical anomalies with a certain scale and considerable intensity are formed especially in NE faults and at the junction of NE and NW faults in the map-sheet.

## 6 Conclusions

The primary dataset of 1 : 50 000 stream sediment survey of Hunjiang City map-sheet, Jilin Province objectively reflects the distribution regularity of elements and the geological and mineral data of the map-sheet. Based on the assessment and ranking of the single-element and integrated anomalies of 16 elements in the map-sheet, a total of 403 single-element anomalies and 24 integrated anomalies of the major metallogenic (indicator) elements were delineated, including three ones of class A and 21 ones of class B. Metallogenic prospect areas and metallogenic target areas were delineated in the map-sheet according to the qualitative evaluation of the resource potential throughout the map-sheet, including one grade I and one grade II metallogenic prospect areas and three level A and seven level B metallogenic target areas. It was ascertained that the deposits in the map-sheet area mainly include meso-epithermal Au, Ag, Sb, Mo, Cu, Pb, and Zn polymetallic deposits. Moreover, two clues of Cu-Pb-Zn-Ag mineralization were discovered through inspection of key anomalies. The geochemical patterns of typical gold and gold–silver deposits in the integrated exploration area were established based on regional mineral features. They serve as important guidance for

future prospecting in the map-sheet area.

The establishment of the dataset provides a set of fundamental data resources of the map-sheet, which can meet the demands of researchers for inquiring the information on stream sediment survey in the map-sheet to a maximum degree. Meanwhile, it creates conditions for sharing of data and resources and provides basic geochemical bases for geological research and applications in other fields.

**Acknowledgments:** The authors hereby extend sincere gratitude to the Development and Research Center of China Geological Survey for their strong support.

#### Notes:

- ① Wang Xuzhong, Liu Jingxia, Qin Honglian, Liu Yulan. 1988. Manual of Geochemical Maps of Hunjiang Map-sheet (11-52-[19])[R]. Jiutai: Institute of No. 5 Geological Survey, Jilin Provincial Bureau of Geology and Mineral Resources. 1–44.
- ② Li Renshi, Xu Man, Li Nan, Ma Jing, Cui Dan, Song Xiaolei. 2013. Report on Achievements of Mineral Resources Potential Evaluation and Geochemical Data Application of Jilin Province[R]. Changchun: Jilin Institute of Geological Survey. 285–326.
- ③ Zhou Xiaodong, Peng Yujing, Lu Xiaoping, Li Dongjin, Wang Guangqi, Pan Jian, Wang Yansheng, Lu Xingbo, Di Xin, Li Fuwen, Yuan Fenghua, Nie Lijun, Zhang Yanling, Cao Limin, Cao Liang. 2019. Annals of Regional Geology of Jilin Province[R]. Changchun: Jilin Institute of Regional Geology Survey.
- ④ Wu Yushi, Wang Haijian, Liu Zhenghong, Che Hailong, Ma Lulu, Li Aaming, Zhao Hongxu, Wang Huiming. 2019. General Report on the Mineral Survey and Prospecting Predication of Integrated Exploration Area of Iron and Gold Deposits in Banshigou, Baishan City, Jilin Province[R]. Tonghua: The Fourth Geological Survey of Jilin Province. 1–328.

#### References

- Chen Bailin, Li Zhongjian, Dong Cheng, Ding Shijiang, Shu Bin, Liao Xiangjun, Dong Faxian, Fu Yangrong. 2004. Ore-controlling structure and its control over gold mineralization in the Baolun gold deposit, Hainan[J]. *Geology in China*, 31(2): 139–146 (in Chinese with English abstract).
- Fu Jianfei, Wang En'de, Xia Jianming, Men Yekai, Chen Huijun, You Xinwei, Cheng Lin. 2014. Element geochemical characteristics and sedimentary palaeoenvironment of the Yanqianshan iron deposit in Liaoning Province[J]. *Geology in China*, 41(6): 1929–1943 (in Chinese with English abstract).
- Guo Fusheng, Wu Zhichun, Xie Caifu, Liu Linqing, Jiang Yongbiao, Shi Guo, Zhou Wanpeng. 2012. Some suggestions for the improvement of the regional geological mapping system and practical skills[J]. *Geology in China*, 39(1): 252–259 (in Chinese with English abstract).
- Hong Xiuwei, Pang Hongwei, Liu Xuewen, LI Erfeng, Wang Wenqing, Wang Changfeng, Liu Tie. 2010. Geological characteristics of the Dataigou iron deposit in Benxi, Liaoning Province[J]. *Geology in China*, 37(5): 1426–1433 (in Chinese with English abstract).
- Li Chaoling, Huang Yuneng, Zhang Kexin, Ye Tianzhu, Li Fengdan, Liu Chang, Long Baolin, Yu Qingwen, Zhang Shenghui, Tao Jixiong, Liu Xiuguo, Ge Mengchun, Lv Zhicheng, Zhu Xueli, Xu Kaifeng, Yang Donglai, Li Jingzhao, Chen Chunxiang. 2013. Database content and structure of solid

- mineral exploration[S]. Beijing: China Geological Survey. 1–319 (in Chinese).
- Li Chaoling, Yang Donglai, Yu Qingwen. 2002. Digital geological survey and mapping techniques[J]. *Geology in China*, 2(2): 213–217 (in Chinese with English abstract).
- Li Suimin, Wu Jingxia, Luan Wenlou, Wei Minghui, Chen Shuqing. 2009. The application of geochemical block method to gold resource assessment in northern Hebei Province[J]. *Geology in China*, 36(2): 444–449 (in Chinese with English abstract).
- Li Suimin, Wei Minghui, Hao Huajin. 2014. The elimination of background influence in the delineation of geochemical anomalies: A case study of geochemical data from Zhangjiakou area[J]. *Geology in China*, 41(6): 2083–2090 (in Chinese with English abstract).
- Liu Hong, Huang Hanxiao, Li Guangming, Xiao Wanfeng, Zhang Zhilin, Liu Bo, Ma Dongfang, Dong Lei, Ma Dong. 2015. Factor analysis in geochemical survey of the Shangxu gold deposit, northern Tibet[J]. *Geology in China*, 42(4): 1126–1136 (in Chinese with English abstract).
- Liu Xun, You Guoqing. 2015. Tectonic regional subdivision of China in the light of plate theory[J]. *Geology in China*, 42(1): 1–17 (in Chinese with English abstract).
- Niu Shuyin, Li Fengyou, Chen Huashan, Sun Aiqun, Wang Baode, Wang Jinzhong, Ma Baojun. 2012. The exploration and prognosis in the depth and the periphery of the Jinchangyu gold deposit in eastern Hebei[J]. *Geology in China*, 39(4): 999–1006 (in Chinese with English abstract).
- Pan Guitang, Xiao Qinghui, Lu Songnian, Deng Jinfu, Feng Yimin, Zhang Kexin, Zhang Zhiyong, Wang Fangguo, Xing Guangfu, Hao Guojie, Feng Yanfang. 2009. Subdivision of tectonic units in China[J]. *Geology in China*, 36(1): 1–28 (in Chinese with English abstract).
- Shi Shujuan, Wang Xueqiu, Gomg Jinzhong. 2011. Statistic relationship between geochemical anomalous areas and gold reserves: A case study of Hebei Province[J]. *Geology in China*, 38(6): 1562–1567 (in Chinese with English abstract).
- Song Xianglong, Xiao Keyan, Ding Jianhua, Fan Jianfu, Li Nan. 2017. Dataset of Major Mineralization Belts of China's Key Solid Mineral Resources[J]. *Geology in China*, 44(S1): 72–81.
- Sun Qizhen. 1994. Marginal mineralization and mineralization marginal effects[J]. *Earth Science Frontiers*, (4): 176–183 (in Chinese with English abstract).
- Wang Denghong. 2016. A discussion on some problems concerning deep exploration of mineral resources in South China[J]. *Geology in China*, 43(5): 1585–1598 (in Chinese with English abstract).
- Wang Laiyun, Sun Nianren, Zhong Liping. 2010. Regional metallogenic geological features of North Daxing'anling precious metals and non-ferrous metals and prospecting method[J]. *Jilin Geology*, 29(1): 36–40 (in Chinese).
- Wang Lei, Hu Zhaoguo, Li Xiangmin, Yan Haizhong, Yang Chao. 2020. Geochemical characteristics of stream sediments and prediction of mining prospects in the Wulandaban–Zhazigou area, Danghe South Mountain, Gansu Province[J]. *Geology in China*, 47(2): 516–527 (in Chinese with English abstract).
- Wang Lei, Yang Jianguo, Wang Xiaohong, Qi Qi, Li Wenming, Jiang Anding, Zhang Zhouyuan. 2016. Geochemical characteristics of stream sediments and prospecting direction in the Shijinpo–Nanjintan area of Beishan, Gansu Province[J]. *Geology in China*, 43(2): 585–593 (in Chinese with English abstract).

abstract).

- Wang Xinchun, Qi Fanyu, Li Xiaolei, Gao Xuezheng. 2016. Research on the geological data integration and service: A case study of geological work in the equipped exploration area[J]. *Geology in China*, 43(2): 691–697 (in Chinese with English abstract).
- Wang Chenghui, Wang Denghong, Huang Fan, Xu Jue, Chen Zhenghui, Ying Lijuan, Liu Shanbao. 2012. The major gold concentration areas in China and their resource potentials[J]. *Geology in China*, 39(5): 1125–1142 (in Chinese with English abstract).
- Wang Yanggang, Li Na, Xiang Yunchuan, Liu Guo, Yu Yan, Zhang Dake, He Cuiyun, He Xuezhou, Zhao Jun, Wu Wenjuan. 2015. The methods and techniques for the construction of the global mineral and resource database[J]. *Geology in China*, 42(1): 342–353 (in Chinese with English abstract).
- Wang Dongbo, Jiang Shaoqing, Dong Fangliu. 2016. Geological exploration of the Rongna porphyry copper deposit in the Duolong ore concentration area, northern Tibet[J]. *Geology in China*, 43(5): 1599–1612 (in Chinese with English abstract).
- Wei Shaogang, Song Yang, Tang Juxing, Gao Ke, Feng Jun, Li Yanbo, Hou Lin. 2016. Geochronology, geochemistry and petrogenesis of quartz diorite porphyrite from the Sena copper (gold) deposit, Tibet[J]. *Geology in China*, 43(6): 1894–1912 (in Chinese with English abstract).
- Wu Yushi, Wang Haijain, Che Hailong, Zhao Hongxu, Ma Lulu. 2020. Primary Dataset of 1 : 50 000 Stream Sediment Survey of Hunjiang City Map-sheet, Jilin Province[DB/OL]. Geoscientific Data & Discovery Publishing System. (2020-12-30). DOI: [10.35080/data.C.2020.P23](https://doi.org/10.35080/data.C.2020.P23).
- Xi Xiaohuan, Li min. 2012. Regional geochemical exploration in China: from 1999 to 2009[J]. *Geology in China*, 39(2): 267–282 (in Chinese with English abstract).
- Xiang Yunchuan, Mou Xuzan, Ren Tianxiang, Liu Rongmei, Wu Xuan. 2018. China Regional Geochemical Exploration Database[J]. *Geology in China*, 45(S1): 41–57.
- Yang Jian, Tang Fawei, Wang Qiao, Wang Yonghua. 2015. Geochemistry and ore-prospecting targeting in Beiya area, Yunnan Province[J]. *Geology in China*, 42(6): 1989–1999 (in Chinese with English abstract).
- Yuan Huixiang, Wang Yanggang, Ren Yongqiang, Wang Chunyy, Liu Na. 2015. Design and development of the information system for integrated exploration on ArcGIS[J]. *Geology in China*, 42(1): 354–364 (in Chinese with English abstract).
- Zhao Wuqiang, Cui Sen, Zou Xianwu, Tang Chaoyang, Xia Jie, Jin Shichao. 2014. Geochemical characteristics of stream sediments and metallogenic prognosis of Heku area, Hunan Province[J]. *Geology in China*, 41(2): 638–647 (in Chinese with English abstract).
- Zhang Jing, Chen Yuanrong, Xie Taoyuan, Li Fengyou, Yuan Yuhua, Zhao Jun, Song Yu, Zou Jie. 2010. A tentative discussion on the genesis, ore-controlling regularity and prospecting direction of the Tuanjiegu gold deposit[J]. *Geology in China*, 37(6): 1710–1719 (in Chinese with English abstract).
- Zhang Jianghua, Wang Kuiying, Zhao Aning, Chen Huaqing, Ke Hailing, Liu Ruiping. 2013. Heavy metal characteristics of stream sediments in the Xiaoqinling gold ore district[J]. *Geology in China*, 40(2): 602–611 (in Chinese with English abstract).
- Zhang Wanyi, Nie Fengjun, Liu Shuwen, Zuo Liyan, Shan Liang, Yao Xiaofeng. 2013. Characteristics

and metallogenic regularities of ore deposits on the western slope of the southern section of the Da Hinggan Mountains metallogenic belt[J]. Geology in China, 40(5): 1583–1599 (in Chinese with English abstract).

Zhang Yongqiang, Tan Le, Li Xiaoming. 2019. The 1 : 50 000 Original Measurement Dataset on Stream Sediments for 7 Map-sheets including the Raofeng Map in the Integrated Survey Area of the Shiquan-Xunyang Gold Ore Zone, Shanxi[J]. Geology in China, 46(S1): 60–71.

Zhang Yunqiang, Chen Haiyan, Zhang Liguo, Chen Chao, Liu Yinglong, He Jiaoyue, Kang Xuan, Zhang Jinlong, Peng Qianpeng. 2015. Geochemical characteristics of stream sediments and metallogenic prognosis of Xinzhangzi area, northern Hebei Province[J]. Geology in China, 42(6): 1980–1988 (in Chinese with English abstract).

Zhi Yunbao, Wang Zenghui, Wei Zhengyu, Zhao Xiqiang. 2019. Geochemical dataset of the 1 : 50 000 Shandong Biguo map-sheet area[J]. Geology in China, 46(S1): 112–124.

Zhu Bingyu, Yang Longbo, Zhu Yiguang, Liu Jiajun, Ma Huadong. 2011. A study of tectonic control of mineralization and geological Indicators for ore-prospecting in the Jinshan (Gold Mountain) gold deposit, Xinjiang[J]. Geology in China, 38(1): 109–118 (in Chinese with English abstract).

Zuo Qunchao, Ye Tianzhu, Feng Yanfang. 2018. Spatial Database of Serial Suite-Tectonic Map-sheets of Mianland China(1 : 250 000)[J]. Geology in China, 45(S1): 1–34.